

## **INFORMATION TO USERS**

**This manuscript has been reproduced from the microfilm master. UMI films the text directly from the original or copy submitted. Thus, some thesis and dissertation copies are in typewriter face, while others may be from any type of computer printer.**

**The quality of this reproduction is dependent upon the quality of the copy submitted. Broken or indistinct print, colored or poor quality illustrations and photographs, print bleedthrough, substandard margins, and improper alignment can adversely affect reproduction.**

**In the unlikely event that the author did not send UMI a complete manuscript and there are missing pages, these will be noted. Also, if unauthorized copyright material had to be removed, a note will indicate the deletion.**

**Oversize materials (e.g., maps, drawings, charts) are reproduced by sectioning the original, beginning at the upper left-hand corner and continuing from left to right in equal sections with small overlaps.**

**Photographs included in the original manuscript have been reproduced xerographically in this copy. Higher quality 6" x 9" black and white photographic prints are available for any photographs or illustrations appearing in this copy for an additional charge. Contact UMI directly to order.**

**ProQuest Information and Learning  
300 North Zeeb Road, Ann Arbor, MI 48106-1346 USA  
800-521-0600**

**UMI<sup>®</sup>**

**Université de Sherbrooke**

**EFFETS DES ÉLECTRONS SECONDAIRES SUR L'ADN**

par

**BADIA BOUDAIFFA**

**Département de Médecine Nucléaire et Radiobiologie**

**Thèse présentée à la faculté de Médecine  
en vue de l'obtention du grade de  
Ph. D. en Radiobiologie  
10 mai 2000**

**© Droits réservés de Badia Boudaïffa**



**National Library  
of Canada**

**Acquisitions and  
Bibliographic Services**

**395 Wellington Street  
Ottawa ON K1A 0N4  
Canada**

**Bibliothèque nationale  
du Canada**

**Acquisitions et  
services bibliographiques**

**395, rue Wellington  
Ottawa ON K1A 0N4  
Canada**

*Your file Votre référence*

*Our file Notre référence*

**The author has granted a non-exclusive licence allowing the National Library of Canada to reproduce, loan, distribute or sell copies of this thesis in microform, paper or electronic formats.**

**The author retains ownership of the copyright in this thesis. Neither the thesis nor substantial extracts from it may be printed or otherwise reproduced without the author's permission.**

**L'auteur a accordé une licence non exclusive permettant à la Bibliothèque nationale du Canada de reproduire, prêter, distribuer ou vendre des copies de cette thèse sous la forme de microfiche/film, de reproduction sur papier ou sur format électronique.**

**L'auteur conserve la propriété du droit d'auteur qui protège cette thèse. Ni la thèse ni des extraits substantiels de celle-ci ne doivent être imprimés ou autrement reproduits sans son autorisation.**

0-612-67095-3

**Canada**

*À mes parents...*

# **TABLE DES MATIÈRES**

## **LISTE DES FIGURES** **III**

## **LISTE DES SIGLES, ABRÉVIATIONS ET SYMBOLES** **VI**

## **RÉSUMÉ**

## **I. INTRODUCTION** **1**

I.1.	PHÉNOMÈNES ULTRA-RAPIDES DE LA RADIATION IONISANTE.....	1
I.2.	ADN: CIBLE PRINCIPALE DES RAYONNEMENTS IONISANTS.....	7
I.2.1.	STRUCTURE DE L'ADN.....	7
I.2.2.	ÉVOLUTION DES ÉVÈNEMENTS APRÈS IRRADIATION.....	7
I.3.	VUE D'ENSEMBLE.....	12

## **II. SYSTÈME EXPÉRIMENTAL** **15**

II.1.	DESCRIPTION DU 1 ER MONTAGE EXPÉRIMENTAL.....	15
II.1.1.	DESCRIPTION GÉNÉRALE DE LA PROCÉDURE.....	15
II.1.2.	ÉVAPORATEUR D'OR.....	17
II.2.	DESCRIPTION DU 2 ÈME MONTAGE EXPÉRIMENTAL.....	19
II.2.1.	CHAMBRE D'IRRADIATION.....	19

**III. RÉSULTATS ET DISCUSSION** **23**

---

III.1. ARTICLE N°1 : Induction of single and double strand breaks in plasmid DNA by 100 to 1500 eV electrons..... 23

III.2. ARTICLE N°2 : Resonant formation of DNA strand breaks by low-energy (3 – 20 eV) electrons..... 62

III.3. ARTICLE N°3 : DNA Damage Induced by Low-Energy (3 – 100 eV) Electrons..... 76

**IV. CONCLUSIONS GÉNÉRALES** **88**

---

**REMERCIEMENTS** **95**

---

**BIBLIOGRAPHIE** **97**

---

## **LISTE DES FIGURES**

Figure 1.1	Événements produits lors du transfert d'énergie de la radiation ionisante à la molécule AB.....	3
Figure 1.2.	Schéma du potentiel d'énergie illustrant l'attachement d'électron resonant à une molécule RH (a). Rendement de désorption de fragments H <sup>-</sup> et représentation de la distribution d'énergie des électrons secondaires d'une particule primaire de 5-150 keV (ou proton en MeV) dans l'eau (cercles ouverts) (b). Représentation de la dissociation dipolaire d'une molécule RH (c) .....	6
Figure 1.3	Structure d'un fragment d'ADN (Faraggi et al., 1995).....	9
Figure 2.1	Vue générale de la chambre d'irradiation.....	16
Figure 2.2	Structure des plaques d'Au(111) analysées par STM (500 nm / 500 nm).....	18
Figure 2.3	Vue générale de la chambre d'irradiation.....	20
Figure 2.4	Porte échantillons.....	21
Figure 3.1	Schéma du porte-échantillon et du canon à électrons.....	30
Figure 3.2	Induction des bris simple, double et multiple par impact d'électrons de 500 eV d'énergie, en fonction du temps d'exposition avec un flux de $5 \times 10^{12}$ électrons/seconde et un débit de dose de 17 kGy/s.....	36
Figure 3.3	Induction de cassures simple, double et multiple par irradiation gamma en fonction de la dose.....	38
Figure 3.4	Perte de plasmides surenroulés et induction de cassures simple et double brins par impact d'électrons et par irradiation gamma en fonction de la dose.....	39
Figure 3.5	Domages de l'ADN en fonction de l'énergie des électrons incidents de 100-1500 eV avec un flux de $5 \times 10^{12}$ electrons/seconde et une exposition de $3 \times 10^{15}$ electrons.....	41

<b>Figure 3.6</b>	<b>Rendements normalisés de la perte des plasmides surenroulés (a) et de l'induction de cassures simple (b), double (c) et multiple (d) par impact d'électrons en fonction de l'énergie.....</b>	<b>42</b>
<b>Figure 3.7</b>	<b>Relation entre la perte des plasmides surenroulés (<math>\ln(S(t)/S_0</math>) et le temps d'irradiation avec des électrons de 500 eV d'énergie (flux de <math>5 \times 10^{12}</math> électrons/seconde et un débit de dose de 17 kGy/s).....</b>	<b>43</b>
<b>Figure 3.8</b>	<b>Schéma réactionnel de la transformation des plasmides d'ADN aux formes surenroulés (S), relaxées (R), linéaires (L) et fragmentés (F).....</b>	<b>44</b>
<b>Figure 4.1</b>	<b>Rendements de cassures doubles (A), simples (B) et perte de plasmides surenroulés (C) en fonction de l'énergie des électrons incidents.....</b>	<b>66</b>
<b>Figure 4.2</b>	<b>Rendements de désorption des fragments <math>H^-</math> induits par impact d'électrons sur des molécules condensées RH = thymine (A), <math>H_2O</math> (B) et tetrahydro-furfuryl alcohol (C).....</b>	<b>69</b>
<b>Figure 4.3</b>	<b>Perte de plasmides surenroulés (A) et induction de cassures simple (B) et double brins (C) par impact d'électrons de 11 eV...</b>	<b>72</b>
<b>Figure 5.1</b>	<b>Rendements de cassures doubles (A), simples (B) et perte de plasmides surenroulés (C) en fonction de l'énergie des électrons incidents.....</b>	<b>81</b>
<b>Figure 5.2</b>	<b>Induction de cassures multiples en fonction du temps d'exposition à 50 eV.....</b>	<b>85</b>
<b>Figure 6.1</b>	<b>Longueur d'onde de l'électron DeBroglie (en Å) en fonction de l'énergie des électrons incidents E (en eV).....</b>	<b>94</b>



## **LISTE DES SIGLES, ABRÉVIATION ET SYMBOLES**

Å	Angstrom.
AD	Attachement Dissociatif.
Ade	Adénine.
ADN	Acide Desoxyribonucléique.
Au(111)	Or avec une orientation 111.
bp	Base Pair (Paire de base).
<sup>60</sup> Co	Cobalt 60.
Cyt	Cytosine.
DD	Dipolar Dissociation (Dissociation Dipolaire).
DEA	Dissociative Electron Attachment (Attachement d'électron dissociatif).
DNA	Deoxyribonucleic Acid
DSB	Double Strand Breaks (Cassure double brin).
EBE	Électrons de Basse Energie.
EDTA	Ethylene diamine tetra-acetate.
eV	Electron-Volt ( = $1.6 \times 10^{-19}$ Joule); meV ( $10^{-3}$ eV); MeV ( $10^6$ eV).
F	Fragmented DNA (ADN fragmenté).
Gua	Guanine.
L	Linear DNA (ADN linéaire).
LET	Linear Energy Transfer (Transfert d'énergie linéique).
LEE	Low-energy electrons (Electrons de basse énergie).
MSB	Multiple Strand Breaks (Cassure de brins multiples).
•OH	Radical hydroxyl.
<sup>32</sup> P	Phosphore 32.
R	Relaxed DNA (ADN relaxé).
S ou SC	Supercoiled DNA (ADN surenroulé).
SSB	Single Strand Breaks (Cassure simple brin).
STM	Scanning Tunneling Microscopy (microscopie de balayage à effet tunnel).
TAE	Tris-Acetate EDTA.
Thy	Thymine.

<b>TMA</b>	<b>Transient Molecular Anion.</b>
<b>Torr</b>	<b>Unité de pression (1 Torr = 1.33 x 10<sup>2</sup> Pa).</b>
<b>UHV</b>	<b>Ultra-High Vacuum (Ultra vide).</b>
<b>UV</b>	<b>Ultra-Violet.</b>
<b>VUV</b>	<b>Vacuum Ultra-Violet.</b>

## **Effets des électrons secondaires sur l'ADN**

**B. Boudaïffa**

*Département de Médecine Nucléaire et Radiobiologie, Faculté de Médecine, Université de Sherbrooke, Sherbrooke, Québec, Canada, J1H-5N4*

Les interactions des électrons de basse énergie (EBE) représentent un élément important en sciences des radiations, particulièrement, les séquences se produisant immédiatement après l'interaction de la radiation ionisante avec le milieu biologique. Il est bien connu que lorsque ces radiations déposent leur énergie dans la cellule, elles produisent un grand nombre d'électrons secondaires ( $4 \times 10^4/\text{MeV}$ ), qui sont créés le long de la trace avec des énergies cinétiques initiales bien inférieures à 20 eV. Cependant, il n'y a jamais eu de mesures directes démontrant l'interaction de ces électrons de très basse énergie avec l'ADN, dû principalement aux difficultés expérimentales imposées par la complexité du milieu biologique.

Dans notre laboratoire, les dernières années ont été consacrées à l'étude des phénomènes fondamentaux induits par impact des EBE sur différentes molécules simples (e.g.,  $\text{N}_2$ ,  $\text{CO}$ ,  $\text{O}_2$ ,  $\text{H}_2\text{O}$ ,  $\text{NO}$ ,  $\text{C}_2\text{H}_4$ ,  $\text{C}_6\text{H}_6$ ,  $\text{C}_2\text{H}_{12}$ ) et quelques molécules complexes dans leur phase solide. D'autres travaux effectués récemment sur des bases de l'ADN et des oligonucléotides ont montré que les EBE produisent des bris moléculaires sur les biomolécules. Ces travaux nous ont permis d'élaborer des techniques pour mettre en évidence et comprendre les interactions fondamentales des EBE avec des molécules d'intérêt biologique, afin d'atteindre notre objectif majeur d'étudier l'effet direct de ces particules sur la molécule d'ADN. Les techniques de sciences des surfaces développées et

utilisées dans les études précitées peuvent être étendues et combinées avec des méthodes classiques de biologie pour étudier les dommages de l'ADN induits par l'impact des EBE.

Nos expériences ont montré l'efficacité des électrons de 3-20 eV à induire des coupures simple et double brins dans l'ADN. Pour des énergies inférieures à 15 eV, ces coupures sont induites par la localisation temporaire d'un électron sur une unité moléculaire de l'ADN, ce qui engendre la formation d'un ion négatif transitoire dans un état électronique dissociatif; cette localisation est suivie d'une fragmentation.

À plus haute énergie, la dissociation dipolaire (i.e., la formation simultanée d'un ion positif et négatif) et l'ionisation jouent un rôle important dans le dommage de l'ADN.

L'ensemble de nos résultats permet d'expliquer les mécanismes de dégradation de l'ADN par les EBE et d'obtenir des sections efficaces effectives des différents types de dommages.

## ***I. INTRODUCTION***

L'utilisation des rayonnements en radiothérapie, ainsi que l'importance de la radioprotection expliquent l'intérêt croissant porté à l'étude des effets de ces agents physiques sur la matière vivante et l'ADN en particulier. En effet, l'interaction des rayons thérapeutiques (X ou Gamma) avec les cellules résulte essentiellement en la génération de l'effet Compton et de l'effet photo-électrique (électrons rapides) qui à leur tour génèrent un nombre important d'électrons secondaires de basse énergie (électrons lents). Par exemple, l'absorption d'un photon de 1 MeV génère approximativement  $4 \times 10^4$  électrons secondaires, dont la plupart ont des énergies bien inférieures à 1 KeV (Platzman, 1955). Il a été aussi démontré par Cobut et ses collaborateurs (1998) que parmi tous les électrons secondaires éjectés dans l'eau, le long de la trace d'un électron primaire de 5 à 150 keV d'énergie initiale (ou d'un proton de quelques MeV), 50 % ont une énergie inférieure à 7.34 eV qui représente le seuil des excitations électroniques dans l'eau (Michaud et al., 1991) ; 56% ont une énergie inférieure à 8.76 eV qui représente un potentiel d'ionisation et 77 % ont des énergies inférieures à 20 eV (la représentation du spectre et la distribution de ces électrons sont représentées sur la figure 3(b) de l'article 3: Electron resonance in DNA induced by very low energy electrons (3 – 50 eV)). Les électrons secondaires peuvent induire donc des excitations électroniques et/ou vibrationnelles, des ionisations ou des dissociations (Sanche, 1991, Nikjoo et Goodhead, 1991). Il serait ainsi crucial d'essayer de comprendre et de décrire les effets des radiations ionisantes par l'étude des événements et processus qu'elles déclenchent lors de leur absorption par le milieu biologique en général et par l'ADN en particulier où sont

produites précisément les modifications les plus importantes quant aux altérations radio-induites.

### ***I.1.- Phénomènes ultra-rapides de la radiation ionisante***

Pour mieux visualiser les événements fondamentaux déclenchés lors de l'absorption des radiations ionisantes, considérons l'exemple d'un système condensé composé exclusivement de molécules diatomiques AB (figure 1).

Le stade primaire comporte l'action directe de la radiation initiale. Au niveau de ce dernier, l'ionisation, la dissociation et l'excitation des molécules AB sont représentées par les réactions 1 à 6.

La majeure partie de l'énergie déposée conduira à la réaction 1 produisant des ions positifs (trous) et des électrons secondaires. Ces derniers ont une énergie bien inférieure à celle de l'électron primaire et leur distribution énergétique se situe majoritairement sous le seuil des 100 eV.

Lorsque l'ion se forme dans un état dissociatif il peut conduire à la réaction 4. Le reste de l'énergie absorbée produit des molécules dans des états d'excitation rotationnelle, vibrationnelle et électronique dont certains seront dissociatifs menant ainsi à la dissociation en fragments neutres ou ioniques (réaction 5 ou 6). Bien sûr, si l'énergie de l'état excité est supérieure au seuil de l'ionisation, la voie 3 devient alors probable et la molécule AB pourra suivre la voie de l'auto-ionisation. À nouveau un électron secondaire pourra être formé.

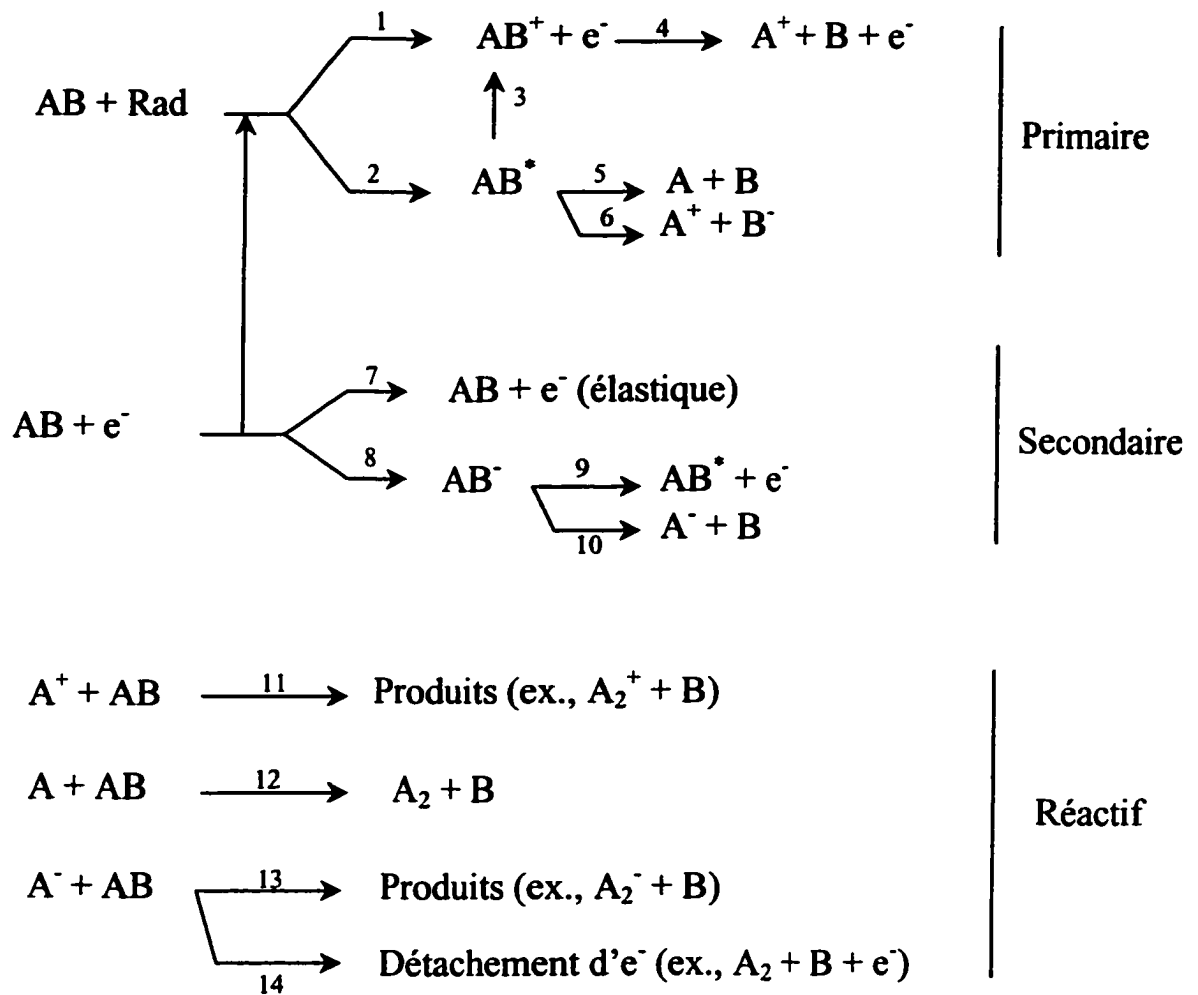


Figure 1.1. : Événements produits lors du transfert d'énergie de la radiation ionisante à la molécule AB.

Les réactions mettant en jeu les électrons secondaires sont abordées dans la deuxième partie de la figure 1. Un électron secondaire pourra interagir élastiquement avec le milieu (réaction 7). Suivant une dépendance énergétique, il pourra participer à l'une des réactions 1-6. Cependant, l'amplitude de probabilité de chacune de ces réactions produites par des électrons secondaires est considérablement différente de celle due aux électrons primaires car la nature ondulatoire de l'électron ne peut être ignorée à basse énergie. L'électron lent perturbe d'une façon marquée les nuages électroniques des molécules avoisinantes. Il peut s'attacher temporairement à une molécule et lui céder une partie importante de son énergie. Ce phénomène appelé "résonance" électronique joue un rôle déterminant dans la compréhension de la déposition d'énergie dans le milieu. En effet, lors de l'interaction résonante, l'électron réside plus longtemps dans le voisinage de la molécule, induit généralement une plus grande distorsion des orbitales moléculaires et un échange d'énergie plus important, comparativement à l'interaction non résonante. Cette perturbation peut engendrer des excitations vibrationnelles ou électroniques (9) et l'attachement dissociatif (10). Dans la matière condensée, à l'énergie de la résonance, ces derniers phénomènes dominent souvent tous les autres causés par des électrons lents. Le temps de vie des ions transitoires ainsi formés se situant généralement entre  $10^{-12}$  à  $10^{-15}$  s, on les considère par ailleurs, comme faisant partie des phénomènes plus rapides que la picoseconde.

Une représentation pratique pour visualiser une résonance est de décrire l'énergie potentielle de la molécule en fonction des distances internucléaires.



La représentation est encore plus simple pour une molécule diatomique où une courbe de potentiel à deux dimensions illustre adéquatement l'énergie potentielle de la molécule neutre, de ses états électroniques et de ses ions négatifs figure 1.2..

En effet, une molécule condensée à basse température est normalement dans son état électronique fondamental et dans son état vibrationnel le plus bas.

La formation d'une résonance est illustrée par le passage de la courbe de potentiel de la molécule neutre à une courbe d'ion négatif dans un temps très court de sorte que la distance internucléaire demeure pratiquement inchangée, c.à.d., la transition s'effectue dans la région du Franck Condon.

L'anion évolue ensuite selon sa nouvelle courbe de potentiel, souvent répulsive dans la région du Frank Condon. Par exemple, la molécule pourra voir ses deux atomes s'éloigner l'un de l'autre. L'autodétachement de l'électron laisse alors la molécule dans un état électroniquement et/ou vibrationnellement excité. Par ailleurs, si le temps de vie de la résonance est assez long pour franchir le point de croisement entre la courbe de l'ion négatif et celle de l'état fondamental de la molécule neutre, la dissociation devient alors, le canal de décroissance possible. Un ou des fragments neutres et un fragment chargé négativement sont formés et on parle alors d'attachement dissociatif (AD).

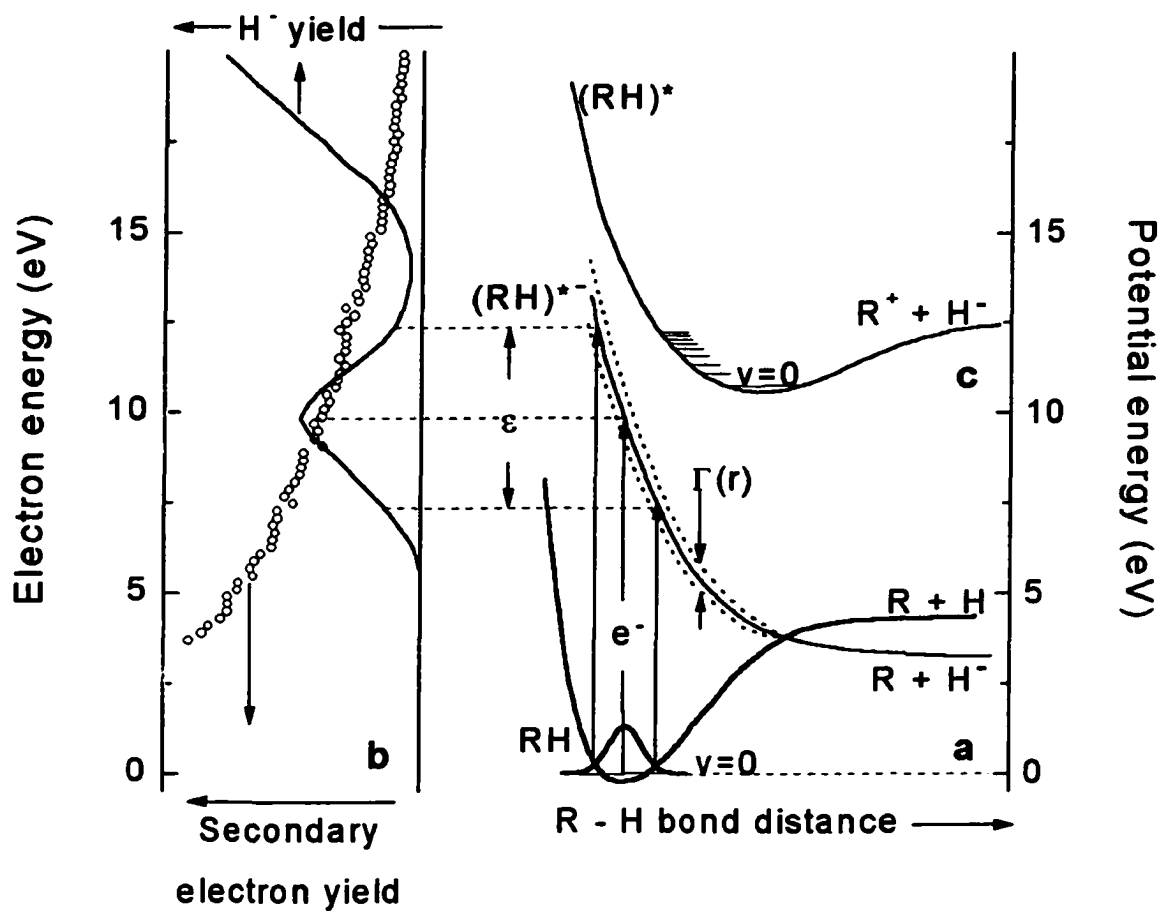


Figure 2.1. : schematic potential energy diagram illustrating resonant electron attachment to a molecule RH (a). Anion fragment yield and calculated relative secondary-electron energy-distributions (b). Dipolar dissociation (c).

Le troisième groupe de la figure 1 (11-14) met en jeu des anions, cations et radicaux neutres créés par des processus dits dissociatifs. Ces radicaux possèdent une énergie cinétique de quelques eV et peuvent réagir rapidement avec le milieu.

On sait par ailleurs que le libre parcours moyen de la majorité des électrons lents varie de 1 à 100Å, ils ont donc le potentiel de produire des dommages localisés dans l'ADN, qui a un diamètre de 20 Å, et lorsqu'autour du nucléosome a un diamètre 100 Å. Il est bien connu aussi que les dommages "localisés" sont les plus difficilement réparables et les plus létaux. Or la plupart des études précédentes ont caractérisé le dommage de l'ADN résultant d'électrons de haute énergie (KeV à MeV), ou d'électrons thermalisés et solvatés, d'ions ou encore de radicaux distribués le long de la trace des radiations et des spurs. En effet, très peu d'études ont été consacrées aux mesures des dommages de l'ADN induits par des électrons secondaires de basse énergie (< KeV). Même si ces investigations peuvent être techniquement difficiles, elles permettent néanmoins de mesurer directement les interactions des électrons secondaires de basse énergie avec l'ADN, qui est l'étape cruciale pour la compréhension de l'effet biologique des radiations ionisantes.

## ***1.2. ADN : Cible principale des rayonnements ionisants***

### ***1.2.1. Structure de l'ADN***

La molécule d'ADN est un polymère formé de deux brins oligonucléotidiques antiparallèles enroulés hélicoïdalement l'un autour de l'autre (double hélice). Chaque brin est composé d'une succession de quatre nucléosides. Un nucléoside est formé par l'une

des quatre bases : *guanine* (Gua), *adénine* (Ade) - bases puriques ; *thymine* (Thy), *cytosine* (Cyt) - base pyrimidiques, liée au 2'-déoxyribose par la liaison N-glycosidique. L'enchaînement des nucléosides est assuré par la liaison phosphodiester entre le carbone 3' et le carbone 5' du nucléoside voisin (Figure 2). L'ordre dans lequel sont disposées les sous-unités constitue le code génétique.

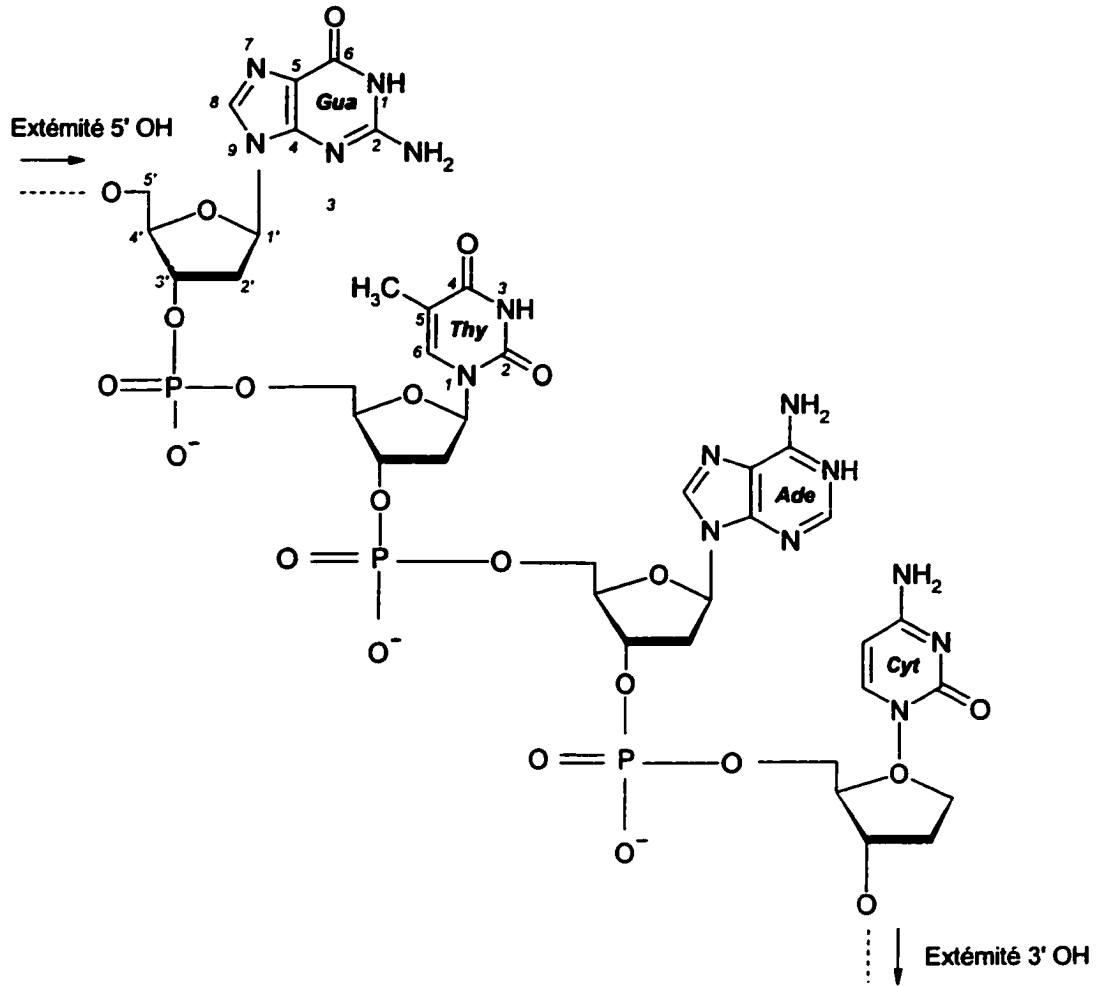


Figure 1.3. : Structure d'un fragment d'ADN (Faraggi et al., 1995)

La stabilité de l'ensemble de la molécule d'ADN est assurée par des liaisons hydrogène entre les bases complémentaires, la thymine s'apparie avec l'adénine et la cytosine avec la guanine. Cette complémentarité rigoureuse permet la duplication de la molécule, chaque brin servant de matrice pour la synthèse du brin opposé. Dans la double hélice, les plans de chacune des bases sont parallèles entre eux et perpendiculaires à l'axe de l'hélice.

A cette structure, s'ajoute une première couche d'hydratation constituée en moyenne de 12 à 15 molécules d'eau associées à chaque nucléotide (formé par l'union d'une base avec un 2'-déoxyribose lui-même attaché à un groupement phosphate) (Swarts et al, 1992). Ces molécules d'eau, fortement liées à l'ADN, accroissent la stabilité de l'ensemble.

Les modifications de la structure chimique des bases nucléiques peuvent conduire à des processus de *mutation*, de *cancérisation* et de *létalement cellulaire*. Ceci a pour conséquence d'altérer le message génétique, rendant, par exemple, inactive la protéine dont la synthèse est dirigée par le gène endommagé. Si la lésion a pour effet de bloquer la réplication de l'ADN, elle peut entraîner la mort de la cellule.

En ce qui concerne les ruptures des chaînes d'ADN (cassures simples et doubles), des fragments formés peuvent être déplacés, par exemple, d'un chromosome à l'autre (une telle réorganisation est appelée recombinaison génétique). Ces fragmentations sont responsables d'*aberrations chromosomiques*, en général très défavorables à la vie de la cellule car elles se traduisent souvent par une perte de l'information génétique portée par les chromosomes ou par de mauvaises interprétations de cette mémoire génétique.

Parce qu'ils modifient les gènes des cellules, les rayonnements ionisants sont qualifiés de ***génétoxiques***.

Dans ce travail, nous nous sommes concentrés seulement sur l'étude des cassures de brins simple, double et multiples.

### ***1.2.2. Évolution des événements après irradiation***

La succession des événements physiques, chimiques, biochimiques et biologiques intervenant après l'ionisation primaire de l'ADN est présentée dans le tableau 1 pour les trois cas : effets direct, quasi-direct et indirect (Becker et Sevilla, 1993 et de Faraggi et ses collaborateurs, 1995).

Temps (s)	Effet direct	Effet quasi-direct	Effet indirect
$10^{-18} - 10^{-13}$	Ionisations et excitations de l'ADN, donnant $\text{ADN}^{+\bullet}$ , $e_{\text{sec}}^-$ et $\text{ADN}^{\bullet}$ .	Ionisations et excitations du milieu proche de l'ADN (eau, complexes ADN/protéines), donnant $\text{H}_2\text{O}^{+\bullet}$ , protéines $^{+\bullet}$ , $e_{\text{sec}}^-$ , $\text{H}_2\text{O}^{\bullet}$ et protéine $^{\bullet}$ .	Ionisations et excitations de l'eau non liées à l'ADN, donnant $\text{H}_2\text{O}^{+\bullet}$ , $e_{\text{sec}}^-$ et $\text{H}_2\text{O}^{\bullet}$ .
$10^{-13} - 10^{-10}$	Thermalisation des électrons. Migration des charges (électron et "trou") et piégeage de celles-ci dans des sites radicalaires dans l'ADN.	Transfert d'une partie des charges ( $e_{\text{sec}}^-$ et "trous") formées vers l'ADN, suivi de processus analogues à ceux produits par l'effet direct. Formation de sites radicalaires dans l'ADN.	Formation des radicaux libres de l'eau ( $\text{OH}^{\bullet}$ , $\text{H}^{\bullet}$ et $e_{\text{aq}}^-$ ). Diffusion de ces espèces et réactions d'une partie de celles-ci avec l'ADN. Formation de sites radicalaires dans l'ADN.
$10^{-10} - 10^{-3}$	Protonation et déprotonation réversibles donnant des radicaux neutres ( $\text{ADN}^{\bullet}$ ) ; addition des ions $\text{OH}^-$ (ou $\text{H}_2\text{O}$ ) avec les cations radicalaires ; formation des pontages ADN-protéines, ADN-ADN ; autres modifications chimiques... Il faut noter que différents effets peuvent conduire à des modifications chimiques identiques.		
$10^{-3} - 10^3$	Evolution des radicaux des fragments osidiques conduisant aux cassures doubles de chaînes d'ADN. Réparation enzymatique des dommages.		
$10^3 - 10^{10}$	Effets sur le développement cellulaire et la réplication. Les cassures doubles de chaînes peuvent provoquer la mort cellulaire, les modifications de bases – mutagénèse, létalité cellulaire ou cancérogénèse.		

Tableau 1 : Evénements produits par l'action du rayonnement ionisant sur l'ADN cellulaire. D'après Becker et Sevilla (1993).

### ***1.3.- Vue d'ensemble***

Les études antérieures dans notre laboratoire ont caractérisé les interactions des électrons secondaires avec des molécules simples (ex.,  $\text{N}_2$ ,  $\text{CO}$ ,  $\text{O}_2$ ,  $\text{H}_2\text{O}$ ,  $\text{NO}$ ,  $\text{C}_6\text{H}_6$ ) et complexes (ex., les hydrocarbures linéaires et cycliques, allant des bases de l'ADN, des



oligonucléotides au plasmides d'AND surenroulé en phase condensée). Il a été possible d'étudier ces interactions en permettant à un faisceau d'électrons de basse énergie de percuter une cible sous des conditions d'hyper-vide. Ces investigations ont démontré que l'impact des électrons de basse énergie peut conduire à des dissociations en fragments moléculaires, atomiques et radicalaires.

Ces études nous ont permis de développer deux nouveaux montages et de nouvelles méthodes pour étudier le dommage, induit par les électrons lents, à l'ADN irradié sous des conditions d'hyper-vide. Nous avons, en premier lieu, étudié l'effet des électrons à des énergies comprises entre 100 et 1500 eV, et pour ce faire, nous avons mis au point un évaporateur d'or afin de fabriquer nous mêmes les surfaces (figure 2.2) sur lesquelles on dépose les cibles d'ADN à irradier. Nous présentons dans l'article n°1 (Induction of single and double strand breaks in plasmid DNA by 100 to 1500 eV) les dommages (assures simple double et multiple) induits par les électrons de 100 à 1500 eV. Une comparaison de ces résultats et ceux obtenus par irradiation  $\gamma$  est aussi présentée. Nous abordons également les problèmes liés au calcul de la dose dans le cas des électrons de basse énergie.

Suite à de nombreux problèmes techniques liés à la préparation des échantillons et au mauvais contrôle du faisceau d'électrons comme mentionné dans l'article n°1, nous avons mis au point un deuxième montage et de nouvelles techniques de préparation des cibles et de traitement des dommages induits à l'ADN, avec un meilleur contrôle du faisceau d'électrons. Les résultats obtenus avec ce dernier montage ont donné lieu à trois articles. Nous présentons dans le premier article (Resonant formation of DNA strand breaks by low energy (3 – 20 eV) electrons), les rendements de bris simple et double brins mesurés

pour la première fois à des énergies plus faibles que le seuil de l'ionisation via des mécanismes de résonance. Dans le second article (DNA damage induced by low-energy (3 – 100 eV) electrons), il est question des cassures multiples induites par impact d'électrons d'énergie comprises entre 3 et 100 eV.

## **II. SYSTÈMES EXPÉRIMENTAUX**

### **II.1.- Description du 1er montage expérimental**

#### **II.1.1.- Description générale de la procédure**

Dans un système à hyper-vide (Fig. 2.1), des échantillons d'ADN sec déposés sur un substrat métallique sont bombardés par un faisceau d'électrons d'intensité et d'énergie variables. Ensuite les échantillons sont retirés du système à vide et analysés par électrophorèse.

Les EBE sont faciles à produire, cependant, la pénétration et la portée limitées de ces particules nécessitent une préparation très stringente des cibles. Il faudrait, en premier lieu, avoir un film mince d'ADN sec, car les molécules se trouvant en profondeur dans un film trop épais peuvent être complètement protégées (Hutchinson, 1954). En second lieu, l'ADN doit être étalé sur une surface conductrice pour pouvoir déterminer le potentiel et l'énergie des électrons incidents et de permettre aux électrons de percuter la cible d'ADN avec une énergie précise. Notre choix pour la surface a été porté sur l'or qui est un métal inerte à 99.9 % de pureté.

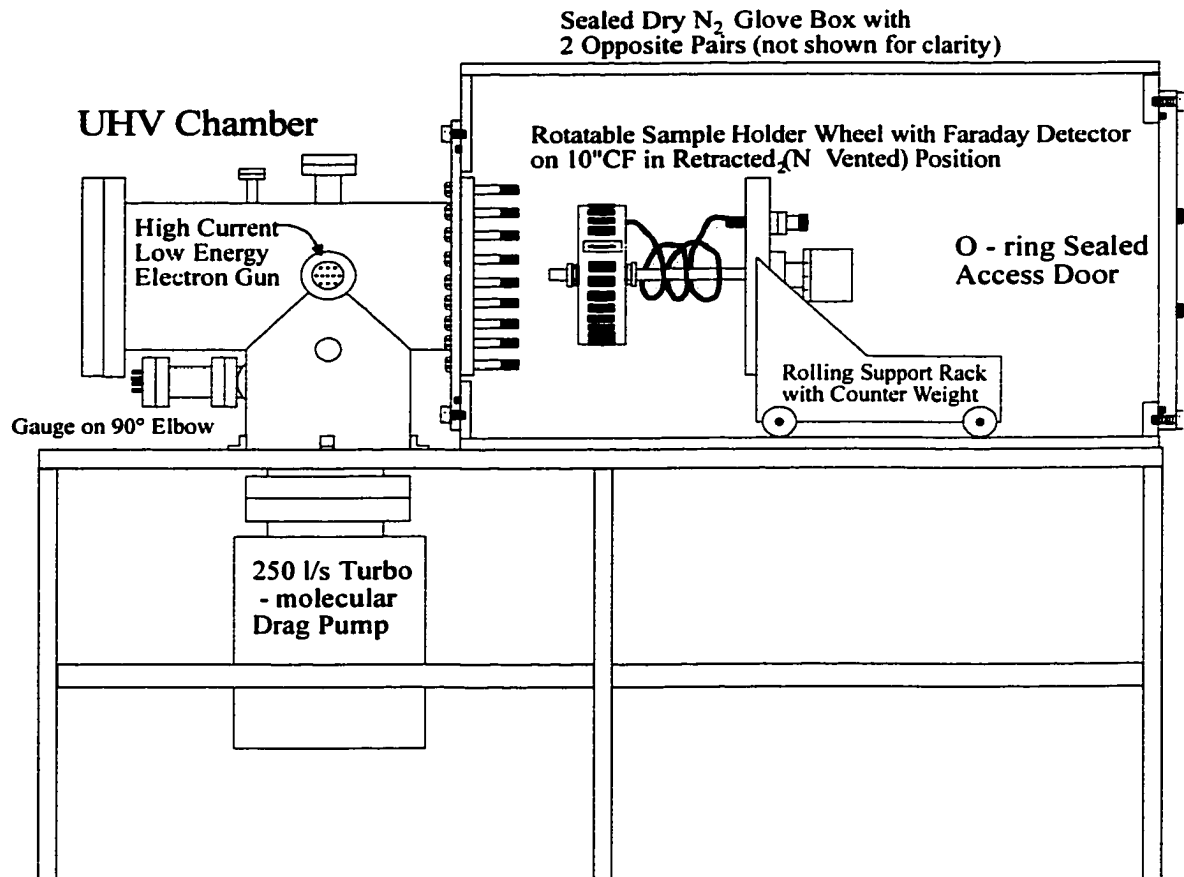


Figure 2.1. : Vue générale de la chambre d'irradiation<sup>1</sup>.

<sup>1</sup> Pour plus de détail, une vue intérieure de la chambre d'ultra-vide est représentés dans la figure 3.1.

### **II.1.2.- Évaporateur d'or**

L'évaporation de l'or s'effectue sur des plaques de verre, dans une cloche à vide ( $\sim 10^{-8}$  Torr) et les plaques peuvent être chauffées pour une meilleure qualité de déposition. Cette chambre à vide permet la production de 60 – 70 plaques d'Or ( $300 \text{ cm}^2$ ) dans les mêmes conditions.

Les plaques de verre chimiquement nettoyées sont placées dans l'évaporateur, après pompage, les plaques sont chauffées pendant 15-20 heures avant l'évaporation de l'Or. La qualité et la structure des plaques d'or sont vérifiées par microscopie de balayage à effet tunnel ("scanning tunneling microscopy"). Ceci donne de larges plans de surfaces (quelques 100 nm), d'orientation (111), avec des échelles atomiques bien visibles (Fig 2.2).

Afin, d'éliminer les contaminations organiques résiduelles, les plaques sont copieusement lavées avec de l'eau distillée et déionisée.

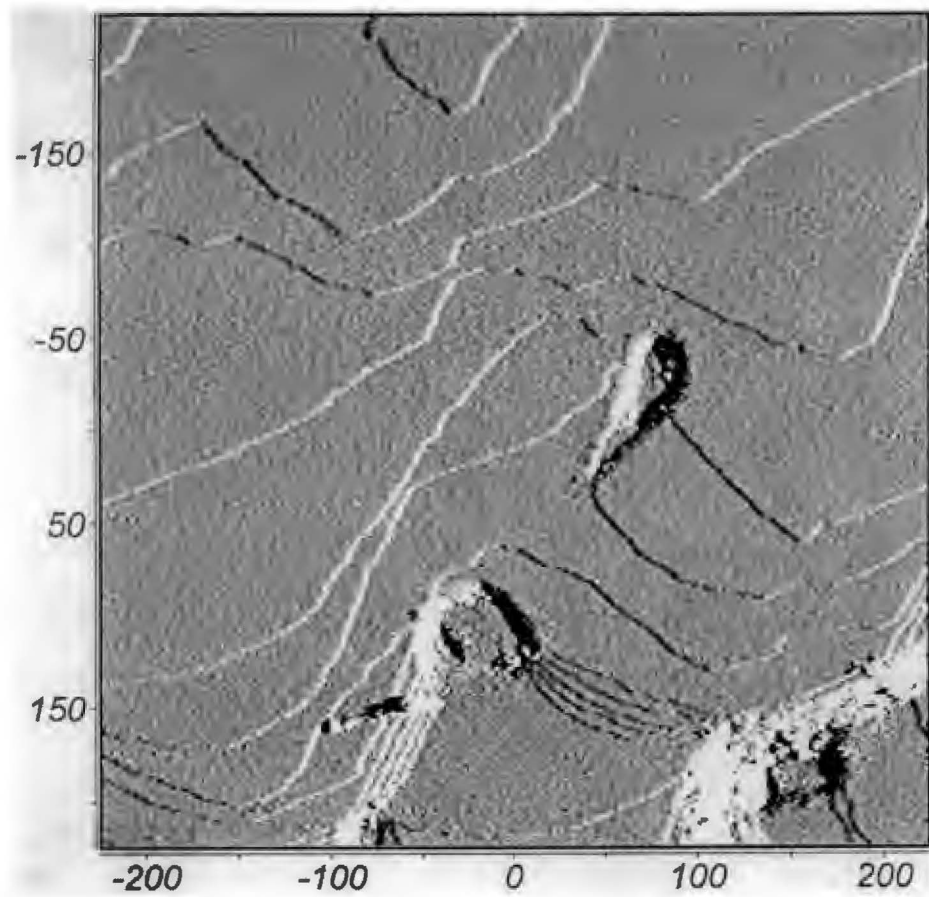


Figure 2.2. : Structure des plaques d'Au (111) analysées par STM (500 nm / 500 nm).

## **II.2.- Description du 2ème montage expérimental**

Nous avons mis au point un deuxième montage pour faciliter la préparation des échantillons dans une atmosphère contrôlée d'azote sec. La surface utilisée dans ce cas est le Tantal. Ce choix a été fait après plusieurs essais de surfaces ordonnées, telles que, l'or, le platine, le molybdène ( $\text{MoS}_2$ ), le tungstène,...etc. En effet, nous avons obtenu de meilleurs résultats et une meilleure reproductibilité avec le Tantal.

### **II.2.1.- Chambre d'irradiation**

Le montage (Fig. 2.3) se divise essentiellement comme suit :

- Une chambre hermétiquement fermée sous atmosphère contrôlée d'azote sec, dans laquelle s'effectue la préparation et la lyophilisation des échantillons. Cette chambre est reliée à un système à vide, muni d'une pompe turbomoléculaire raccordée à une pompe à vide primaire. La pression typique dans cette partie de l'appareil est d'environ  $10^{-10}$  Torr.
- Un canon à haut courant (0-50  $\mu\text{A}$ ), de basse énergie (0 – 100 eV) constitué d'un filament de tungstène thorié comme source d'électrons, de lentilles pour former et focaliser le faisceau d'électrons. Le faisceau d'électrons orienté par un champs magnétique, quitte le monochromateur (D) pour percuter le film condensé sur la cible (L).

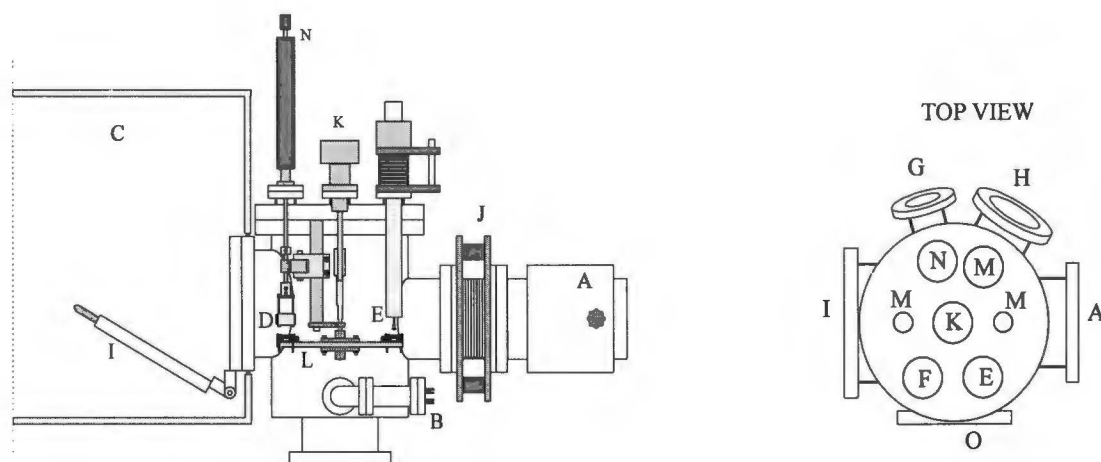


Figure 2.3. : Vue générale de la chambre d'irradiation. A: Pompe turbo-moléculaire (520 l/s); B: Jauge ionique; C: Boite à gants fermée hermétiquement; D: Canon d'électrons; E: Sonde Kelvin; F: Fenêtre; G: Analyseur de gaz résiduel (RGA); H: Fenêtre; I: Porte d'accès; J: soufflet Anti-vibration; K: Commande de rotation; L: Porte échantillons; M: Alimentations électriques; N: Commande linéaire; O: Fenêtre.



- Un porte échantillons sur lequel sont placées les cibles devant être bombardées (fig. 2.4).

- Une cage de Faraday muni d'une fente de 0.33mm permet de mesurer la densité et la distribution spatiale du faisceau d'électrons. Des plaques phosphorescentes ont été aussi utilisées afin de visualiser et de contrôler la distribution des électrons sur les cibles d'ADN.

Le nombre d'électrons percutant l'échantillon par unité de temps est calculé à partir de la fraction du courant total incident qui atteint le dépôt

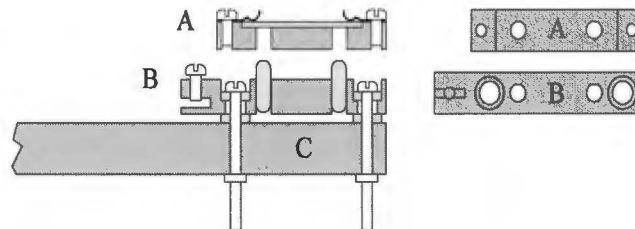


Figure 2.4. : Porte échantillons. A: Support à échantillons avec feuille de Tantal, B: Porte échantillons fixé sur un plateau horizontal tournant.

Les cibles sont introduites et placées sur le porte échantillons de la chambre UHV afin d'être irradiées sous un vide de  $\sim 10^{-8} - 10^{-9}$  torr.

La grosseur du faisceau d'électrons est visualisée et évaluée grâce aux feuilles de Phosphore qui fluorescent lors de l'interaction de cette dernière avec les électrons. Ceci nous permet ainsi d'orienter le faisceau d'électrons, grâce au champs magnétique, et de l'étaler, grâce aux lentilles, afin d'obtenir une surface de bombardement recouvrant toute la surface de l'ADN déposé.

Avant d'introduire les cibles, la chambre UHV incluant le porte échantillons peut être dégagée à 100°C.

### **III. RÉSULTATS ET DISCUSSION**

***III.1. ARTICLE N°1 : Induction of single and double strand breaks in plasmid DNA by 100 to 1500 eV electrons. In press. Int. J. Rad. Biol. 2000.***

INDUCTION OF SINGLE AND DOUBLE STRAND BREAKS IN PLASMID DNA BY 100 TO 1500

eV ELECTRONS

**Badia Boudaïffa, Darel Hunting, Pierre Cloutier, Michael A. Huels and Léon**

**Sanche**

**Canadian Medical Research Council Group in the Radiation Sciences, Dept. of Nuclear Medicine and Radiobiology, Faculty of Medicine, University of Sherbrooke, Québec, Canada J1H 5N4**

***ABSTRACT***

Dry supercoiled plasmid DNA was irradiated with electrons of energies ranging from 0.1 to 1.5 keV and the results were compared with those obtained by  $\gamma$ -irradiation of the same plasmid in solution. For electron irradiation, the plasmid is deposited on a gold substrate under a controlled atmosphere to minimize contamination of the DNA film. Electron bombardments are performed under ultra high vacuum (UHV –  $10^{-9}$  Torr) conditions. DNA damage is detected by gel electrophoresis followed by quantitation of the DNA bands by fluorescence or by hybridization with a radioactive probe. Our results show that electrons within the energy range of the secondary electrons generated by high-energy ionizing radiation induce single, double and multiple double strand breaks in DNA. For equal doses, we observe a marked increase in the efficiency of induction of double and multiple strand breaks in supercoiled DNA as a function of electron energy. In contrast to  $\gamma$ -irradiation, the formation of small DNA fragments by electrons does not seem to be related to the production of the linear form of the plasmid. We also discuss problems associated with low-energy electron irradiation experiments and dose calculations in thin films.

## ***INTRODUCTION***

The interaction of diagnostic and therapeutic x-rays or gamma rays with cells results essentially in the generation of Compton recoil and photo-electrons (fast electrons) which in turn generate large numbers of low energy electrons (slow electrons) (Uehara and Nikjoo, 1996). For example, the absorption of a 1 MeV photon generates approximately  $4 \times 10^4$  secondary electrons, most of which having energies well below 1 keV (Platzman 1955). These electrons may induce electronic and/or vibrational excitations, ionizations or dissociations (Sanche, 1991, Nikjoo and Goodhead, 1991). Subsequent chemical reactions result in the DNA damage characteristic of ionizing photons, such as single and double strand breaks (von Sonntag, 1987), and oxidative damage to the bases (Fuciarelli *et al.* 1990), resulting mainly from hydroxyl radical formation (Miliigan *et al.* 1993). Since the inelastic mean free path of the majority of secondary electrons varies from 1 to 100 Å (Marsolais *et al.* 1991; Pimblott and LaVerne 1995; Bass and Sanche 1998), they have a high probability of depositing energy in clusters, producing complex damage in DNA (Nikjoo and Goodhead, 1989; Goodhead, 1990), which may be responsible for a major part of the biological effectiveness of low-LET radiation (Goodhead and Nikjoo, 1990). It is believed that clustered DNA damage is the most difficult to repair and thus the most lethal (Ward 1981, 1985). Most previous studies have characterized the DNA damage resulting from either high-energy electrons, with energies in the keV to MeV range, or thermalized and solvated electrons, and thermal ions and radicals distributed along the radiation tracks and spurs. However, very few studies have endeavoured to measure the DNA damage which can be induced by low energy secondary electrons, in the sub-keV energy range (Folkard *et al.*, 1993). Although these investigations may be technically demanding, they should allow us to directly

measure the interactions of low energy secondary electrons with DNA, a crucial step towards understanding, and ultimately controlling, the biological effects of ionizing radiation.

It is possible to study the damage induced by low energy secondary electrons in various biological target molecules by means of a beam of electrons with energies varying from 1 eV to 1 keV (Hutchinson, 1954; Cole, 1974; Folkard et al. 1993; Dugal et al. 1999). Previous studies have characterized such damage for simple (e.g. N<sub>2</sub>, CO, O<sub>2</sub>, H<sub>2</sub>O, NO; Kimmel et al, 1995; Sanche 1997, Bass *et al.* 1998) and more complex molecules; e.g., linear and cyclic hydrocarbons (Kelber and Knotek, 1982; Rowntree *et al.* 1991a, 1991b) as well as DNA bases (Huels *et al.* 1998) and small single stranded oligonucleotides (Dugal *et al.* 1999) in the condensed phase. These investigations have demonstrated that low energy electron (LEE) impact can lead to molecular dissociation, i.e. to the production of atomic and radical ions and fragments.

LEE experiments on insulating materials (e.g., biological, organic and molecular solids) must usually be performed with thin films condensed or deposited on a metal substrate in order to avoid charging of the target (Sanche 1997). Since LEE have short mean free paths (Tougaard and Chorkendorff, 1987), it is also necessary to minimize surface contamination during the experiment. In other words, the prepared surface must be atomically clean and kept clean, before and during the measurements. This is usually accomplished by introducing the sample in the vapor phase, into an ultra-high vacuum (UHV) system, and allowing the target molecules to condense on a clean metal substrate. Afterwards, the induced damage is monitored *in vacuo* by techniques of microanalysis such that the sample is never exposed to atmospheric contaminants. UHV techniques of microanalysis such as electron stimulated desorption, temperature-programmed

desorption and electron-energy loss, UV photoelectron and X-ray photoelectron spectroscopies are highly sensitive and therefore it is possible to monitor LEE-induced damage with very small amounts of material; e.g., by analyzing an area of a few mm<sup>2</sup> on films having thicknesses ranging from 1 to about 5 nm. Thus, due to the high conductivity of the metal substrate and the small film thickness, the molecular solid target does not charge appreciably during the time required to measure the induced damage. Under these conditions, the electron energy remains well defined within the beam resolution.

Unfortunately, large biomolecules usually cannot be vaporized without decomposition. Furthermore, when the probed damage cannot be assessed under UHV conditions, the sample must then be both prepared and analyzed outside the UHV environment. Since *ex vacuo* techniques are usually less sensitive, more degraded material must be prepared by electron bombardment, a condition which may be difficult to meet for thin films and highly focused LEE beams. Thus, new methods of analysis must be devised if we are to perform such experiments with an accuracy and reliability similar to those performed in vacuum on thin condensed films. We are presently developing this type of technology for measurement of LEE-induced damage within pure samples prepared and analyzed outside UHV.

The analysis of single and double strand breaks induced by LEE impact on DNA represents a typical experiment, in which both target preparation and analysis must be performed outside an UHV environment. In this article, we describe our first attempt to develop an apparatus and the methodology to determine the damage induced by LEE in supercoiled plasmid DNA, irradiated under UHV conditions. As in the case of simpler molecules, we require that the target be clean (i.e., pure) and thin. In order to insure

sample purity, the samples are deposited onto UHV-prepared gold substrates, under a pure dry nitrogen atmosphere in which they are lyophilized before transfer into an UHV chamber. Subsequently, the samples are irradiated with a beam of monochromatic electrons. The apparatus has capabilities for irradiation between 100 and 1500 eV. In the present study, we show that secondary electrons of energies from 0.1 to 1.5 keV induce single, double, and multiple double strand breaks in supercoiled plasmid DNA. In addition,  $\gamma$ -rays were used as a positive control to generate strand breaks in the same plasmid, thus allowing a comparison of the formation and interconversion of the three topological forms of the plasmid. Finally, our results are compared with published results obtained with soft X-rays,  $\gamma$ -rays and 25-4000 eV electrons on similar targets irradiated under different conditions. This study has allowed us to better define the problems associated with LEE irradiation of high molecular weight nucleic acids; namely, difficulties associated with the stability of pure supercoiled plasmid DNA in UHV, the relatively small amount of material which can be irradiated and the dosimetry associated with LEE irradiation of thin films.

## ***MATERIALS AND METHODS***

### ***A. Preparation of supercoiled plasmid DNA and metal substrate***

We use gold as substrate films since they are relatively inert and easy to prepare by evaporation onto glass or mica. High-purity gold (99.99 %) is evaporated onto either freshly cleaved mica or glass slides, degassed at 350° C or 150° C, respectively, in an UHV chamber held at  $10^{-8}$  Torr. The quality of the gold substrates is verified by scanning tunneling microscopy. The substrate gold surfaces consist of azimuthally disordered large surface planes (several hundred nanometers) of crystalline Au(111).



Plasmid DNA is prepared from pGEM3Zf(-) (1399 bp; Promega), amplified in *E. coli* (DH5 $\alpha$ ) and extracted by alkaline lysis. The supercoiled form of the plasmid is purified using an anion exchange resin (Qiagen), following the manufacturer's protocol. The plasmid is precipitated and re-dissolved in nano-pure water and stored frozen.

### *B. Preparation of DNA onto gold substrates*

All sample manipulations are carried out in a hermetically sealed glove box under a dry nitrogen atmosphere. This glove box is attached and sealed directly to the UHV chamber to allow sample transfer without exposure to air. The Au substrates are cooled to  $-80^{\circ}$  C and 25  $\mu$ l of DNA solution in ultra-pure water containing 500 ng of plasmid are deposited, covering an area of about 25 mm<sup>2</sup>. The DNA is then lyophilized using a hydrocarbon-free sorption pump. The thickness of the DNA is estimated to be about 10 nm (density of DNA of about 1.35 g.cm<sup>-3</sup>) assuming minimal (less than 20 %) clustering of the plasmids in the solid. Although we have not experimentally confirmed the conformations of the DNA molecules in our target solids, electron microscopy studies have shown that supercoiled plasmids adopt a plectonemic form when deposited on carbon grids (Cozzarelli *et al.* 1990; Vologodskii 1992). In plectonemic supercoiled plasmids (i.e. inter-wound DNA as opposed to solenoidal or toroidal DNA) the DNA winds up and back down a super-helical axis, thus creating many sites where the DNA helix crosses itself or is in close proximity to another part of the same DNA molecule. Thus the 10 nm thick solid is estimated to consist on average of about 5 layers of plasmid DNA.

The samples are fixed to the rotary wheel shown in figure 1 and introduced into an UHV chamber previously degassed by heating to 100 $^{\circ}$  C under vacuum for 3-4 days. Afterwards, the UHV chamber is evacuated for ca. 24 hours by a hydrocarbon-free

pumping system consisting of a primary turbo-molecular drag pump (250 l/s) followed by a carbon vane fore pump. The chamber reaches a pressure of  $10^{-9}$  Torr after pumping for 24 hrs.

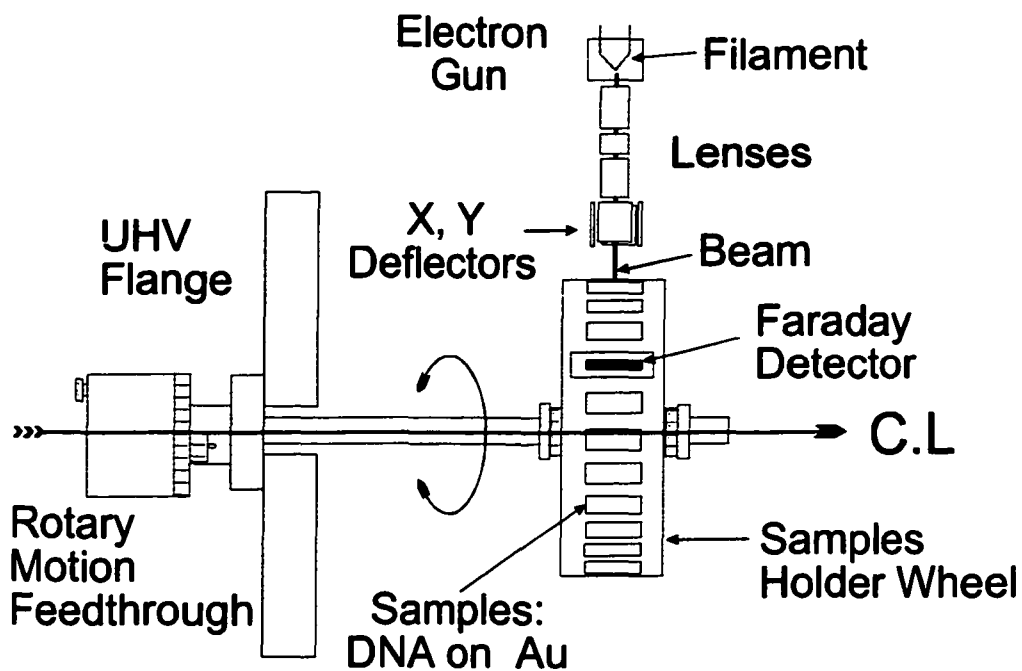


**Figure 1:** View of rotatable sample holder and low energy electron gun.

### *C. LEE and $\gamma$ -ray irradiation.*

The UHV chamber is equipped with a high current (0-50  $\mu$ A, 0.5 eV resolution) electron source, covering the energy range of 100-1500 eV. The incident electron beam is collimated with a coaxial magnetic field; as shown in Figure 1, electric fields in the x and y direction are applied to the electron beam for scanning the beam across the sample. In the present experiments, the beam was scanned at a frequency of 100 Hz over an area much larger than that covered by the DNA sample, in order to ensure that all the DNA was irradiated. The number of electrons incident on the target DNA was determined from the area scanned by the beam and the area occupied by the DNA. DNA damage by LEE can be expressed as a function of the exposure,  $\epsilon$ , the total number of electrons which have arrived at the target solid of area A (5 mm diameter on average) after a fixed time t of irradiation; thus  $\epsilon = JtA$ , where J is the flux-density (number of electrons  $s^{-1} cm^{-2}$ ). The details of the rotatable sample holder are shown in Figure 1. One position on the holder is occupied by a Faraday detector slit (0.33 mm by 5 mm) which allows measurements of the spatial distribution of the electron beam. Irradiation times with a beam current of 1  $\mu$ A were varied between 10 and 90 min. In order to generate positive control samples containing single, double and multiple double strand breaks, plasmid DNA samples in solution are exposed to a graded series of doses of ionizing radiation in a  $^{60}Co$   $\gamma$ -ray source (Gammacell 220 irradiator, Nordion Inc., Canada).

### *D. Determination of DNA damage and dosimetry*

Following electron irradiation, the samples are re-dissolved in Tris-EDTA buffer (pH 7.5). Then samples which have been  $\gamma$ -irradiated or electron bombarded are electrophoresed on a 1% agarose gel in TAE running buffer. The gel is soaked in a

solution of ethidium bromide (1  $\mu\text{g/ml}$ ) and photographed with a digital camera, allowing quantification of the different topological forms of the plasmid (supercoiled, nicked circle, linear and short linear). In some cases, the DNA is transferred to positively charged nylon membranes (Hybond N<sup>+</sup> ; Amersham) and hybridised with a <sup>32</sup>P labelled probe, prepared using random priming on the plasmid template, as described by Maniatis *et al.* (1982). The radioactivity is then quantified using a PhosphorImager (Molecular Dynamics). Several types of DNA controls are produced, including DNA in solution (prior to lyophilisation), lyophilized DNA held in dry N<sub>2</sub> and lyophilized DNA held under UHV, but not irradiated with electrons. The electron beam results are expressed in terms of DNA damage as a function of electron energy and dose or time of electron irradiation at a given electron current, i.e., exposure. In all cases, the dose rate is provided in the figure captions such that time can be converted to dose. Finally, aliquots of solution of  $\gamma$ -irradiated samples are analyzed in the same manner and the results are expressed as a function of dose.

The damage induced by LEE on thin films is usually measured in terms of the number of specific fragments or breaks per incident electron or similar units, such as an effective cross section for a given target (Leclerc *et al.*, 1987; Sanche 1995). Although such definitions provide values which are significant for beam experiments on thin targets, they do not allow easy comparison with the results of other experiments which are expressed per unit of absorbed energy (or dose) by the target. Ideally, one would like to be able to calculate from available cross sections and stopping powers the energy absorbed by the thin film during the time of bombardment. However, such calculations are bound to provide unrealistic values, since the deposited energy from the portion of the incident electron beam which interact with the film constituents is not retained within the film. It is known, for thin films (1-5 nm) on metal substrates, that within picoseconds most of the

electronic and vibrational energy deposited in the film at the instant of the interaction is transferred to the metal substrate via exciton motion followed by quenching on the metal (Zimmerer, 1988) and coupling of intramolecular vibrations to phonon modes of the substrate (Cavanagh, 1994). Furthermore, part of the incident electron energy is directly deposited in the metal substrate via image-charge interactions (Gomer, 1975) and most of the prompt photons from decay of excited states are emitted in vacuum and in the substrate.

To demonstrate this point, we can calculate, based on the thin film approximation, the rate of energy deposition in the first DNA layer of our film. For a thin target of thickness  $\Delta x$ , bombarded by an electron current of intensity  $I_0$ , during time  $t$ , with an energy  $E$ , the total amount of energy absorbed by the target,  $\Delta W(E)$ , may be written as the sum of the energies absorbed  $\Delta w(E, E_p)$  by each process leading to an energy loss  $E_p$  while the beam traverses the target.

$$\text{i.e.} \quad \Delta W(E) = \sum_{p=0}^n \Delta w(E, E_p) \quad [1]$$

$$\text{where} \quad \Delta w(E, E_p) = I_0 Q(E, E_p) E_p t \Delta x \quad [2]$$

where  $Q$  is the scattering probability per unit length. Substituting [2] into [1], we obtain,

$$\Delta W(E) = t \Delta x I_0 \sum_{p=0}^n Q(E, E_p) E_p = t \Delta x I_0 S(E) \quad [3]$$

in which the stopping cross section  $S(E) = \sum_{p=0}^n Q(E, E_p) E_p$  related to the stopping powers by a density factor (Kimura et al., 1993). Within a first approximation, we assume that this thin layer approximation is valid for energy deposition within a first layer of DNA (i.e., through a diameter of  $\sim 20 \text{ \AA}$ ). In this case, the instantaneous energy

deposited or instantaneous dose to the first layer can be calculated; the subsequent layers will necessarily absorb less energy. Dose calculation for the entire film would require the use of multiple scattering theory (Michaud and Sanche, 1987) with a good knowledge of cross sections and angular distributions within condensed DNA. Taking the stopping power calculated by Laverne and Pimblott (1995) in dry DNA, we obtain for 500 eV electron energy, a dose rate of about 17 kGy/s to the first layer. This means that for irradiation times typical of those of the present experiment (e.g., 10 min), the first layer of DNA would have received about  $10^7$  Grays. Assuming that all this energy remains in the film, we can calculate the effective temperature at long times from Debye's model of specific heat (Ashcroft and Mermin, 1976). Taking tabulated values of Debye's temperatures and specific heats from the latter reference, we find an unrealistic value of the order of  $10^5$  degrees Kelvin for the effective temperature of the first layer. Even if we assumed that the entire film would absorb a hundred times less energy per unit mass, it would have decomposed and evaporated during the experiment.

Another problem in assigning a dose only to the DNA sample arises from secondary electrons created in the metal substrate which return to the thin film, where they may cause damage. Obviously, the film cannot simply be considered in isolation since, in these experiments, energy is imparted to the film-substrate system, which is the effective target. A more realistic dose calculation should therefore include the portion of the substrate which has received energy from the beam. This is also difficult to estimate, but as a first approximation, we can assume that beam energy is deposited within the extrapolated ranges of the electrons in the substrate-film system. Since energy quickly flows out of the extrapolated range, this approximation also overestimates the dose delivered to the substrate-film system but it is more comparable to that measured in

conventional bulk experiments. Taking the extrapolated ranges for DNA and gold given in the work of Iskef et al. (1983), we find that the present results were obtained at a dose rate of about 50 Gy/s at 500 eV. This means, for example, that for a 10 min irradiation at 500 eV a dose of 30 kGy has been delivered to the target. According to this estimate, we must therefore consider that the present LEE-results were obtained at high doses. With the present apparatus and methodology, the use of considerably smaller doses resulted in amounts of measured forms of DNA which were within the statistical fluctuations of the control samples; i.e., those which were transferred into UHV but not irradiated. We also note that within this calculation of energy absorbed by the substrate-DNA system, the absorbed dose becomes dependent on extrapolated electron ranges which are themselves inversely proportional to the stopping powers.

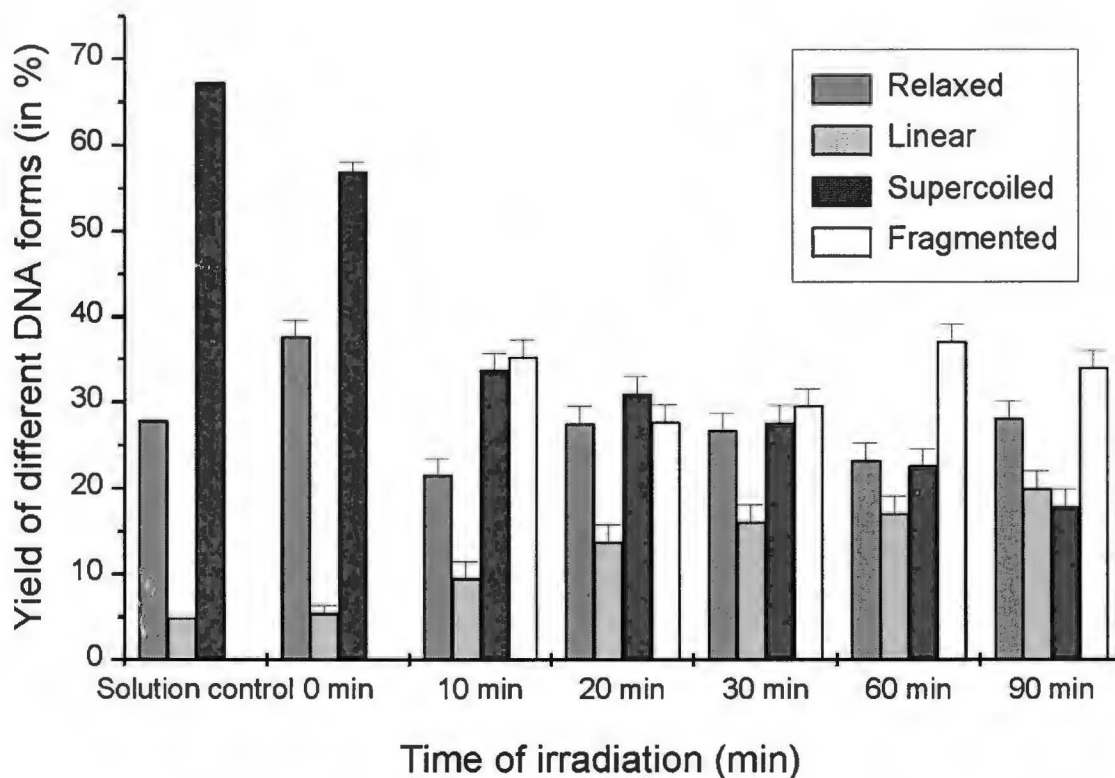


**Figure 2:** Induction of single, double and multiple double strand breaks in plasmid DNA by a beam of 500 eV electrons as a function of irradiation time (i.e. exposure) for a flux-density of about  $5 \times 10^{12}$  electrons/second and dose rate of about 17 kGy/s.



## **RESULTS**

The induction of DNA damage by 500 eV electrons as a function of irradiation time (i.e. exposure) is shown in Figure 2. Each point represents an average of five independent measurements. The error bars correspond to the spread in the data. The plasmid (pGEM3Zf(-)) in solution, prior to deposition on the gold substrate, consists of approximately 70% supercoiled (S) molecules, less than 5% linear (L) and about 25% relaxed circular (R) molecules (Figure 2; solution control). Deposition, lyophilization and re-dissolution of the plasmid results in the induction of some further single strand breaks (SSB) but no double strand breaks (DSB) (Figure 2; 0 min irradiation). Irradiation of the lyophilized plasmid under UHV with 500 eV electrons (flux-density of about  $5 \times 10^{12}$  electrons/second-cm<sup>2</sup>) leads to further loss of the supercoiled form and to the formation of three forms of the plasmid: relaxed circular, full length linear and short linear fragments, resulting from the generation of single strand breaks, double strand breaks and multiple double strand breaks, respectively. The short linear plasmid fragments appear as a smear following agarose gel electrophoresis indicating that they are of random lengths. Within experimental error, the amount of linear plasmid increases linearly with irradiation time up to 30 min, while the amount of supercoiled plasmid decreases.

For comparison, the induction of strand breaks in an aqueous solution of plasmid as a function of dose of  $\gamma$  rays is shown in Figure 3. Each point corresponds to three independent measurements. The error bars represent the spread in these data. Under  $\gamma$ -ray irradiation, both the relaxed and linear forms of the plasmid increase as a function of radiation dose, while the supercoiled form decreases. As observed with 500 eV electrons irradiation,  $\gamma$  irradiation also induces formation of short linear DNA fragments (i.e. multiple double strand breaks) but only at the highest doses, (Figure 3; 300 Gy). The short

linear DNA fragments increased as a function of radiation dose for doses higher than 300 Gy (not shown). To facilitate comparison, the percentages of the different forms of the plasmid as a function of dose are presented in Fig. 4(a-c) for low energy electrons (taken from Fig. 2) and in Fig. 4(d-f) for  $\gamma$ -rays (taken from Fig. 3).

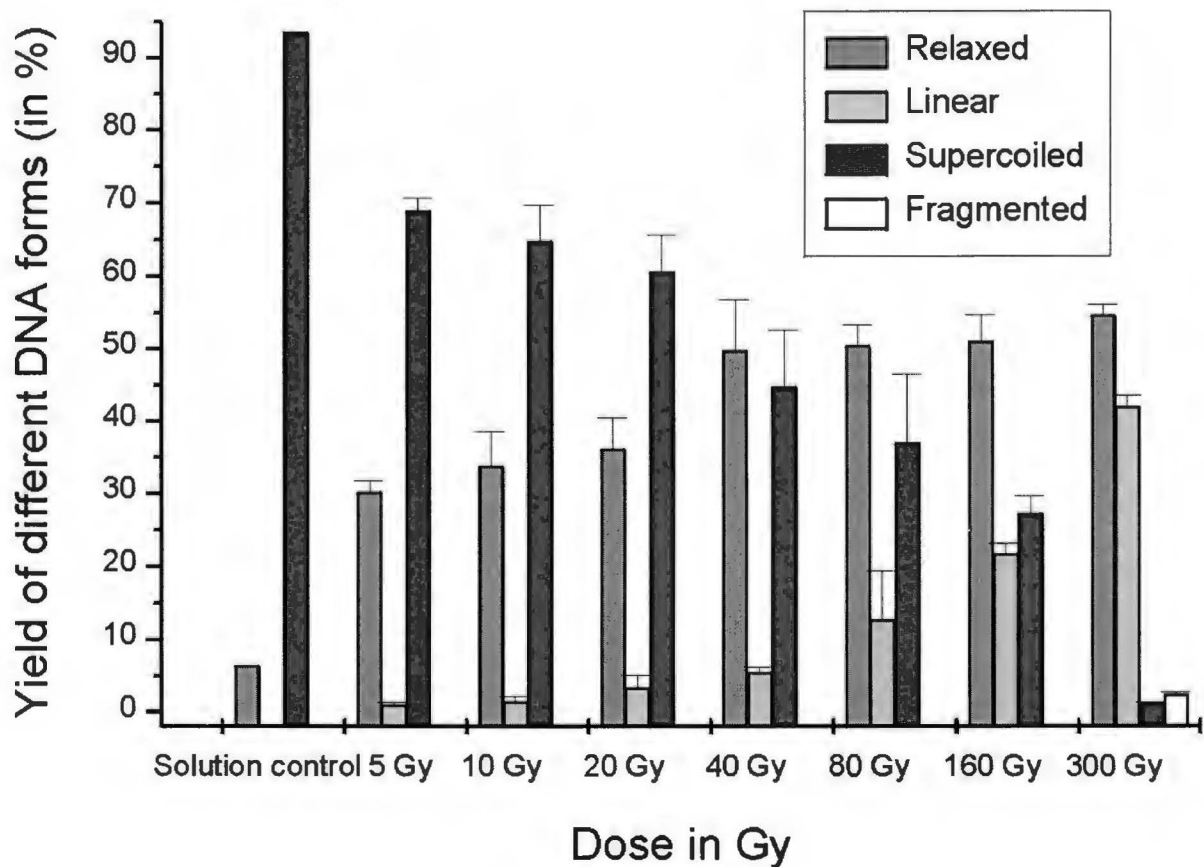


**Figure 3:** Induction of single, double and multiple double strand breaks in plasmid DNA by gamma rays as a function of dose.

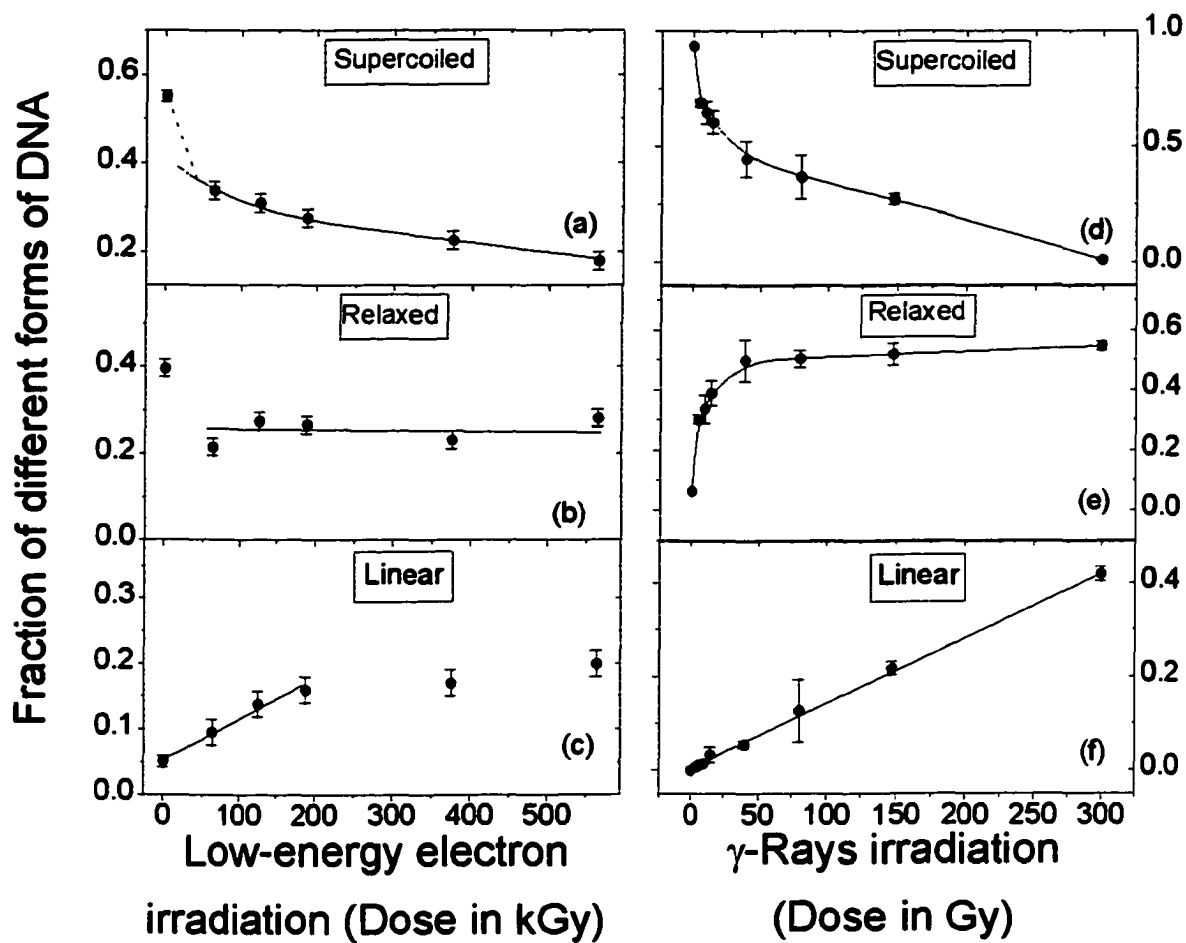


**Figure 4:** Loss of supercoiled and induction of single and double and breaks in plasmid DNA by low-energy electron and gamma rays irradiation as a function of dose.

The induction of DNA damage as a function of incident electron energy, for energies ranging from 100 to 1500 eV, is shown in Fig. 5, for a flux-density of about  $5 \times 10^{12}$  electrons/second-cm<sup>2</sup> and a time irradiation of 10 min. (i.e., an exposure to  $3 \times 10^{15}$  electrons). The dose rates calculated from corresponding extrapolated ranges appear in the scale on top. The results indicate that for equal exposures, the efficiency of forming multiple double strand breaks increases as a function of incident electron energy. For example, 100 eV electrons converted approximately 10% of the DNA to short linear fragments while an equal exposure to 1500 eV electrons converted approximately 50% of the DNA to short linear fragments. When strand breaks are expressed in terms of yield per adsorbed dose this increase is even more significant and the linear form is clearly found to increase with electron energy, while the relaxed configuration remains constant. This is shown in Fig. 6, where the percentage of the different forms present after irradiation have been normalized to the 500-eV dose and plotted as a function of electron energy.

The relationship between the loss of supercoiled DNA (S(D)) and the exposure is shown in Fig. 7, for the data on 500 eV electrons taken from Fig. 2. Since, at a fixed energy, the absorbed energy dose is proportional to the exposure, one can see from Fig. 7 that the loss of supercoiled plasmid in thin films can be defined by the typical dose-response relation:

$$S(D) = S_0 \exp(-D/D_0)$$

where, D represents the dose,  $D_0$  a constant expressed in dose units and  $S_0$  the initial percentage of supercoiled DNA in the unirradiated sample.

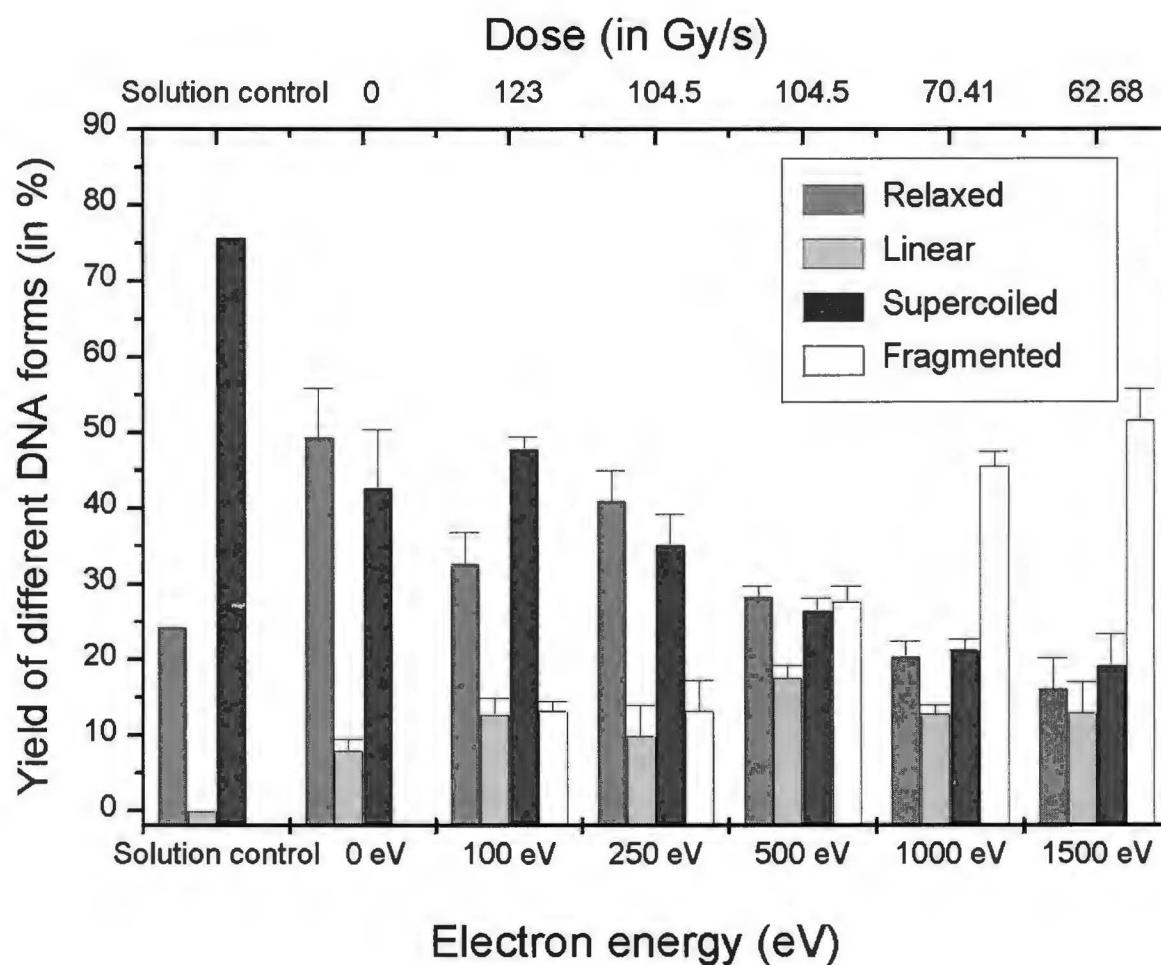


**Figure 5:** Induction of damage in plasmid DNA as a function of incident electron energy, from 100 to 1500 eV, for a flux-density of about  $5 \times 10^{12}$  electrons/second and a exposure of  $3 \times 10^{15}$  electrons.

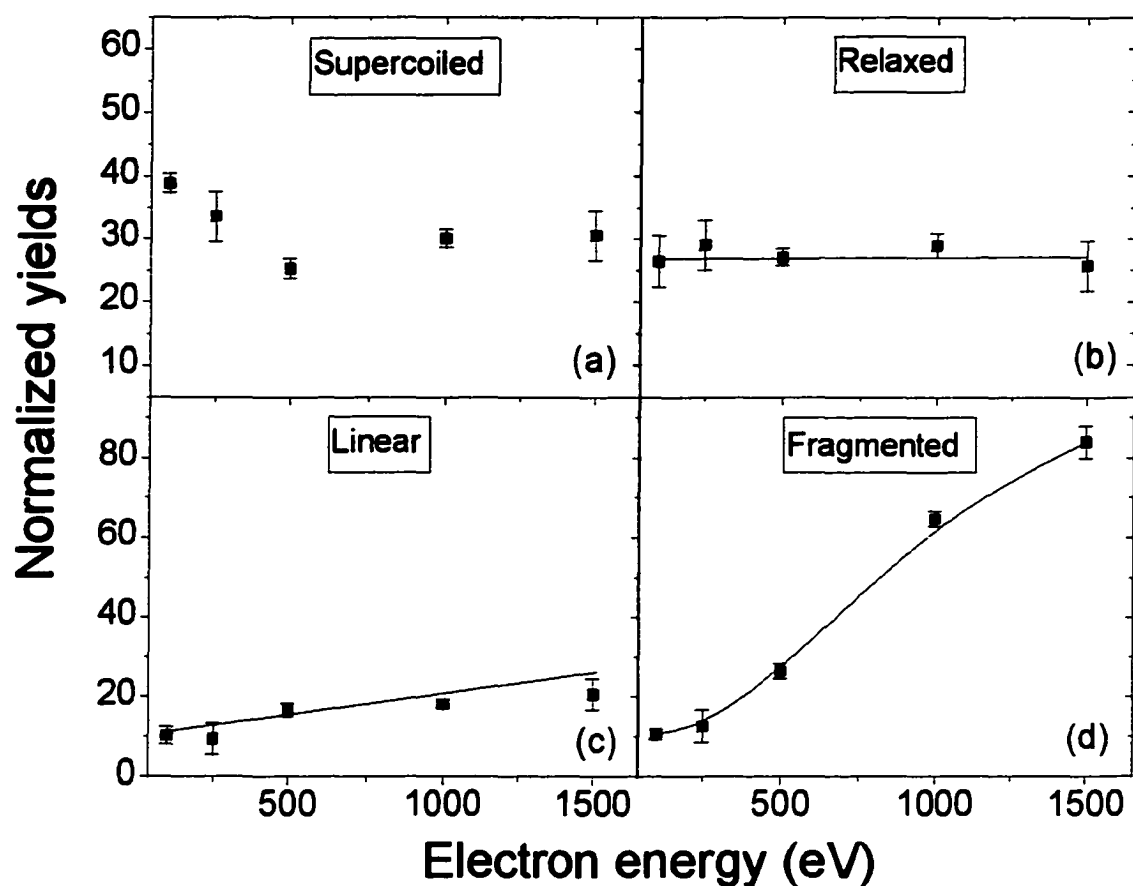


**Figure 6:** Normalized yields of the loss of supercoiled (a) and the induction of single (b), double (c) and multiple double (d) strand breaks in plasmid DNA by electrons as a function of energy.

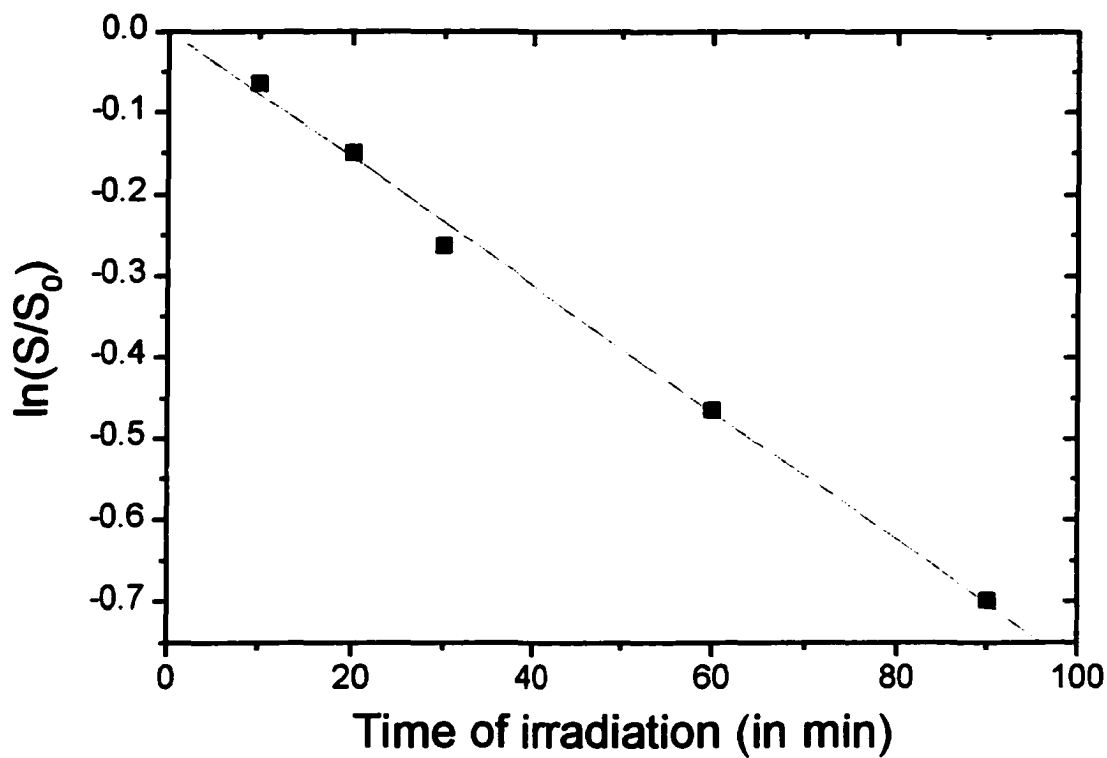


**Figure 7:** The relationship between the loss of supercoiled plasmid ( $\ln(S(t)/S_0)$ ) and time of irradiation with 500 eV electrons (for a flux-density of about  $5 \times 10^{12}$  electrons/second and dose rate of about 17 kGy/s).

## **DISCUSSION**

In this section, we discuss our results in terms of the reaction pathways leading to the different forms of plasmids. These are shown in Fig. 8, where S, R, L and F represent the configurations supercoiled, relaxed, linear and fragmented, respectively.

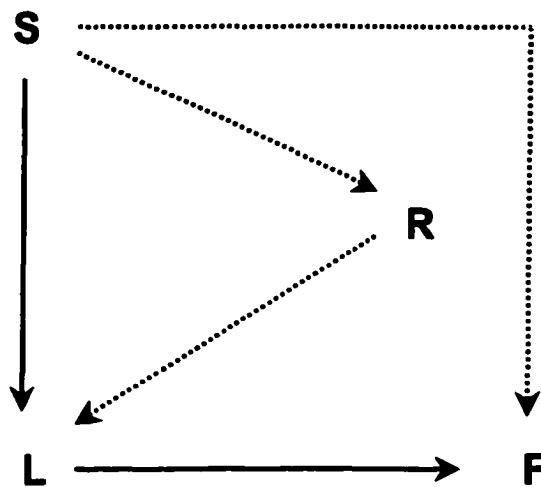


**Figure 8:** Reaction scheme for the transformation of the DNA plasmid to its different forms, where S, R, L, and F represent supercoiled, relaxed circular, linear and short linear fragments, respectively.

### *A. Gamma irradiation*

Irradiation of the plasmid by gamma radiation results in the direct conversion of supercoiled DNA to the relaxed circular and linear forms. However, beyond a dose of about 30 grays, the yield of the relaxed form (Fig. 4e) saturates and reaches a steady state. Since beyond 30 grays the amount of supercoiled DNA continues to decline and the yield of the linear form continues to rise, it appears that the quantity of relaxed plasmid



produced from the supercoiled form equals that which is depleted by conversion to linear plasmid. Since the yield of linear plasmid is a linear function of dose (Fig. 4f), it is clear that the gamma rays have an equal probability of producing a double strand break from the two substrates (supercoiled and relaxed plasmid) at high doses. The possibility of two independent single strand breaks occurring in close proximity is considered to be negligible at these doses, given the length of the plasmid. If the probability of forming a double strand break was different for the relaxed and supercoiled forms, then the dose-response relationship for the formation of linear DNA would deviate from the linear. For example, if the relaxed form were less susceptible, the formation of linear DNA as a function of dose would decline as the percentage of relaxed DNA increased. The short linear DNA fragments probably result from the introduction of a second double strand break in full length linear molecules by another interaction, given that the short DNA molecules are observed mainly at the highest dose, when all supercoiled plasmids have been already converted to other forms.

This interpretation is consistent with the results of Spothem-Maurizot *et al.*, 1990, which also show a decrease in the amount of the supercoiled form, an increase in that of the circular relaxed form, and an increase in the amount of the linear form upon  $\gamma$ -irradiation of plasmid DNA. Similar to our results, they show a linear dose-response relationship for the production of the linear form while the yield of the circular form saturates. The linear dependence was also reported by Frankenberg-Schwager *et al.* (1980), Chaterjee and Magee (1985), and Frankenberg-Schwager (1989) for different types of radiation. Siddiqi and Bothe (1987) have concluded that the gamma-induced double strand breaks which depend linearly on dose are formed from an initial single strand break by a mechanism of radical transfer to the opposite strand.

### ***B. LEE irradiation***

The results in Figure 4(c) show that, up to an estimated dose of 200 kGy, the percentage of linear DNA increases linearly as a function of the exposure to the LEE beam. On the other hand, the percentage of relaxed circular plasmid remains relatively constant, between 22 and 28% of the total, throughout the irradiation. A priori, this linear relationship with dose suggests that the supercoiled form may be directly converted to the linear form as a result of the formation of a double strand break by a single electron. This hypothesis is consistent with the fact that 500 eV electrons have a short mean free path, thus increasing the probability of an interaction with both DNA strands and generating a double strand break. This is supported by the hypothesis of Frankenberg (1971), that DNA double strand breaks are mainly produced by blobs (i.e., energy depositions up to 500 eV in volumes  $\leq 30$  nm).

The appearance of the short DNA fragments at short times of irradiation in Fig. 2 may be due to the relatively high LEE dose. In the case of  $\gamma$ -irradiation (Fig. 3), such fragments only occur at doses 300 Grays and above. The difference with LEE irradiation, however, is that the short length linear DNA appears at relatively high levels well before the complete conversion of the supercoiled plasmid to other forms, as in the case with  $\gamma$ -irradiation. In addition, these small fragments are formed during LEE irradiation before substantial accumulation of linear DNA has occurred. These results suggest that DNA multiple fragmentation dynamics with LEE is different from that with  $\gamma$ -rays. We have attempted to perform preliminary experiments at lower doses with more samples and have observed the same results, i.e., formation of short fragments even at early times (10 seconds), with 100 eV electrons (flux-density of about  $2.5 \times 10^{12}$  electrons/second, and dose rate of about 50 kGy/s). Thus, these results seem to indicate that at least a portion of the

fragments arise from multiple sites of damage by a single electron. On the other hand, comparing the results in Figures 2-4, for SSB and DSB formation we find that  $\gamma$  and LEE irradiation of the plasmid produce similar behavior as a function of dose; i.e., the level of the relaxed form quickly saturates (Fig. 4b,e), the linear form increases as a linear function of the dose (Fig. 4c,f) and the depletion of supercoiled DNA occurs exponentially (Fig. 4a,d), as is also illustrated by the dose response curve shown for 500 eV electrons in Fig. 7. However, in the case of LEE irradiation, the relaxed form saturates immediately after the minimum dose and the linear form does not exhibit a linear behavior with dose beyond exposure of 30 min (i.e., a dose of 200 kGy). Thus, assuming similar dose behaviors, this would mean that, as estimated in section 3, the doses imparted to DNA are much larger with LEE than with  $\gamma$ -rays. Another aspect of these results which indicates that high doses have been delivered to the DNA sample is seen in Figure 4a (i.e. the rapid decline in the percentage of supercoiled DNA after 10 min of irradiation). The similarity between both types of radiation is surprising, since breaks in plasmid DNA  $\gamma$ -irradiated in solution have been attributed to OH radical attack (Spotheim-Maurizot *et al.*, 1990 and references therein), whereas in LEE experiments the direct and quasi-direct effects should be operative. On the other hand, double strand breaks by low LET radiation are believed to result from the effect of LEE having energies in the range studied here. So, in that respect, similar behavior is expected from these different particles. In fact, comparison of the yields of DSB's produced by  $\gamma$ -ray photons in supercoiled DNA irradiated in the dry versus the aqueous state produces the same linearity with dose (Ito *et al.*, 1993).

The results normalized for equal doses shown in Fig. 6 indicate that for equal amounts of absorbed energy within the substrate-film "target", the damage induced by electrons in the range of 100-1500 eV varies considerably. Since soft X-ray irradiation

can produce electrons having energies from 0.1 to keV's, some correspondence should exist between our results and those obtained with monochromatic photons of narrow bandwidth (Hieda et al. and citations therein). Indeed, the synchrotron radiation results of Hieda et al (1994) show that between 0.1 and 2 KeV the yields of SSB's and DSB in pBR322 DNA exhibit a behavior similar to that seen in Fig. 6(b) and (c), respectively. On the other hand, in direct electron beam experiments also performed at high doses. Folkard *et al.* (1993), found that from 50 to 2000 eV, the efficiency of conversion of supercoiled DNA (predominantly due to the production of SSB) as well as the yield of DSB's increased with increasing electron energy. As seen in Fig. 6(a) and (c), their results agree with those of the present experiment. However, beyond 500 eV we do not observe as they did, any further increase in the conversion of SC DNA to other forms. According to Folkard et al., their results are consistent with calculations showing that the absolute number of small energy depositions within the DNA, per unit dose (of the type that can cause a single strand break but not a double strand break) increases with increasing incident electron energy (Nikjoo et al., 1991).

Although multiple damage by multiple electron interactions undoubtedly occurs with the present doses, interaction at different energies must have different effects in order to explain the results in Fig. 6(c) and (d). The drastic increase in the number of short fragments shows that the higher energy radiation is more efficient at producing multiple strand breaks. If these multiple breaks were only the result of many single breaks induced by isolated and not correlated events on the same plasmid, we would have to conclude that, at higher energies, electrons are more efficient in producing single breaks. However, this is not the case; in Fig. 6(b) the relaxed form is seen to be constant with electron energy. Thus, the increase in the linear (Fig. 6(c)) and fragmented (Fig.

6(d)) forms with energy suggests that, as the electron energy increases from 0.1 to 1.5 keV, single hits by LEE become more efficient in producing double and multiple strand breaks. Since the latter grows faster with energy than double strand breaks, some events must be directly producing multiple strand breaks. These results are not too surprising in view of the ability of high LET radiation to produce local multiple damage as discussed by Ward (1985) and Goodhead (1994). However the increase seen in Fig. 6(c) and (d) cannot be directly related to LET or stopping power since 1-1.5 keV electrons have lower stopping powers than those of lower energy (Pimblott *et al.*, 1996). Since 1-1.5 keV electrons have longer range, they and the secondary electrons produced have a greater probability of reaching other sections of DNA, outside the local volume of initial energy deposition, where they would cause further local multiple damage and hence multiply damaged DNA. As calculated by Pimblott *et al.* (1996), in H<sub>2</sub>O the effective range of a 100 eV electrons is about 5 nm. Such a short interaction distance is efficient at producing DSB but not multiple fragmentation. Similar conclusions are reached from the calculations of Mikhalik and Frankenberg (1996). These authors show that electrons with initial energies between 200 and 500 eV are the most effective for producing DSB's, reflecting their efficiency at concentrating deposited energy in the nanometer volumes of a target consisting of the DNA double helix with some associated bound and bulk water molecules. It was also shown by Paretzke, 1987; and by Mikhalik 1993, that electrons with these energies produce clusters of deposited energy in the nanometer range. According to their effectiveness in producing double strand breaks, Mikhalik and Frankenberg, 1996, classified the energy transfers into two groups, - energy transfers leading to low-energy electrons with initial energies between 200 and 500 eV inducing preferentially complex DSBs, and - energy transfers yielding electrons of less than about

200 eV, producing at least two ionizations, generating mainly simple DSB (Mikhalik *et al.* 1994, 1996). The possibility of inducing double strand breaks in DNA by either photons (Lehmann and Ormerod, 1970; Kampf *et al.*, 1977; Frankenberg-Schwager *et al.*, 1979, Michael *et al.* 1994) or high-energy ionizing radiation (Corry and Cole, 1968; Blöcher, 1982; Boon *et al.* 1984; Seddigi *et al.* 1987; Krisch *et al.* 1991) or low-energy electrons (Folkard *et al.*, 1993) as the result of single events is now well established, but it has also been shown that double strand breaks can result from multiple events (Ward 1981; Krisch *et al.* 1991; Prise *et al.* 1993).

Finally, we note that, in the present experiments, the formation of multiple double strand breaks in a DNA molecule by single LEE would be enhanced if regions of the DNA which are distant in primary sequence along the DNA double strand are in close contact. This is the case in plectonemically supercoiled DNA (i.e. interwound DNA as opposed to solenoidal or toroidal DNA) in which the DNA winds up and back down a superhelical axis, thus creating many sites where the DNA helix crosses itself or is in close proximity to another part of the same DNA molecule. Thus, the deposition of sufficient energy in a small volume by low energy, high LET electrons could result in the formation of two double strand breaks which are separated by hundreds of base pairs along the primary sequence.

## **CONCLUSIONS**

We have developed an apparatus and the methodology to allow irradiation of pure plasmid DNA with 100–1500 eV electrons. The first results obtained with electrons in this range were reported in this article. Despite technical difficulties related to the preparation of pure stable supercoiled DNA, reasonable statistics in the measured yield of the different

forms could be obtained at high doses for electron bombarded samples under UHV conditions. Induction of single, double and multiple double strand breaks were clearly observed but analysis of the dose response remained complex. We found an increase in the efficiency of inducing double and multiple strand breaks in supercoiled DNA as a function of electron energy. This increase has been related to the energy dependence of stopping powers and larger penetration depth of secondary electrons produced by the higher-energy primary electrons.

It is obvious from the present study that improvements in the experimental technique, as well as the UHV apparatus, are required in order to obtain results at significantly lower doses or exposures. These are necessary to obtain more precise information about the mechanisms of electron induced DNA damage, and particularly at lower incident electron energies even down to a few eV. Using the experimental insight gained in the present study, we have recently begun such work on a second generation UHV apparatus; although it permits measurements at much lower electron beam intensities, it is currently operating in incident electron energy in the 0 – 20 eV range. However, initial results obtained with this device on the effects of 3 – 20 eV electrons are promising (Boudaïffa *et al.*, 2000), and indicate that further improvements should result in a better understanding of the mechanisms of genotoxic damage by medium energy (100 – 1500 eV) electrons.

Calculations of the dose absorbed by a thin film of organic matter is also a problem that should be addressed in future research on LEE damage. In this article, we have opted to consider a portion of the substrate as the "target" in which energy is absorbed in order to obtain a realistic value for the energy absorbed by the DNA sample. That portion of the substrate was defined by extrapolated ranges for 1.0-1.5 keV electrons. Since at energies

lower than 0.1 keV such extrapolations are difficult, we may have to eventually generate all the inelastic cross sections below 100 eV, if we are to investigate this energy range with a reasonable level of confidence. We have generated such cross sections for amorphous H<sub>2</sub>O films (Michaud and Sanche, 1987, 2000; Bader *et al.*, 1988) and are presently extending our measurements to organic molecules.

**Acknowledgements:** This work was supported by the Medical Research Council of Canada and the Health and Safety Program of the CANDU Owners' Group (COG).



## **REFERENCES**

- Ashcroft N. W., and Mermin N. D., 1976, Solid State Physics, Chapt. 23. Holt Saunders, Philadelphia.
- Bader G, Chiasson J., Caron L. G., Michaud M., Perluzzo G. and Sanche L., 1988, Absolute scattering probabilities for subexcitation electrons in condensed H<sub>2</sub>O. *Radiation Research* 114, 467-479.
- Bass A. D. and Sanche L., 1998, Absolute and effective cross-sections for low-energy electron-scattering processes within condensed matter. *Radiation Environment Biophysics*, 37, 243-257.
- Blöcher D., 1988, DNA double-strand break repair determines the RBE of  $\alpha$ -particles. *International Journal of Radiation Biology*, vol. 54, No. 5, 761-771.
- Boon P. J., Cullis P. M., Symons M. C. R. and Wren B. W., 1984, Effects of ionising radiation on deoxyribonucleic acid and related systems. Part 1. The role of oxygen. *Journal of the Chemical Society: Perkin Transactions II*, 1393-1399.
- Boudaïffa, Cloutier, Hunting, Huels, and Sanche, Resonant induction of DNA strand breaks by low energy (3 – 20 eV) electrons, *Science* (2000, in press).
- Cavanagh R. R., Heilweil E. J. and Stepheson J. C., 1994. Time-resolved measurements of energy transfer at surfaces. *Surface Science* 299/300, 643-655.
- Chatterjee A., and Magee J. L., 1985, Theoretical investigation of the production of strand breaks in DNA by water radicals. *Radiation Protection Dosimetry*, 13, 137-140.

- Cole A., Cooper W. G., Shonka F., Corry P. M., 1974, DNA scission in Hamster cells and isolated nuclei studied by low-voltage electron beam irradiation. *Radiation Research*, **60**, 1-33.
- Corry P. M., and Cole A., 1968, Radiation-induced strand scission of the DNA of mammalian metaphase chromosomes. *Radiation Research*, **36**, 528-543.
- Cozzarelli N. R., Boles T. C. and White J. H., 1990, Primer on the topology and geometry of DNA supercoiled, in DNA topology and its biological effects, edited by N. R. Cozzarelli and J. C. Wang (Cold Spring Harbor Laboratory Press).
- Dugal, P. C.; Huels, M. A.; Sanche, L., 1999, Low-energy (5-25 eV) electron damage to homo-oligonucleotides. *Radiation Research*, **151**, 325-333.
- Folkard M., Prise K. M., Vojnovic B., Davies S., Roper M. J. and Michael B. D., 1993, Measurement of DNA damage by electrons with energies between 25 and 4000 eV. *International Journal of Radiation Biology*, **64** (6): 651-658.
- Frankenberg D., 1971, Direct and indirect radiation effect in yeast cells, in *Proceedings of the 3<sup>rd</sup> Symposium on Microdosimetry*, 289-301.
- Frankenberg D., Goodhead D. T., Frankenberg-Schwager M., Harbich R., Bance D. A. and Wilkinson R. E., 1986, Effectiveness of 1.5 keV aluminium K and 0.3 keV carbon K characteristic X-rays at inducing DNA double-strand breaks in yeast cells. *International Journal of Radiation Biology*, **50**, N° 4, 727-741.
- Frankenberg-Schwager M., 1989, Review of repair kinetics for DNA damages induced in eucaryotic cells *in vivo* by ionising radiations. *Radiotherapy and Oncology*, **14**, 307-320.

- Frankenberg-Schwager M., Franckenberg D., Blocker D., and Adamczyk C. 1980, The linear relationship between DNA double strand breaks and radiation dose (30 MeV electrons) is converted into quadratic function by cellular repair. *International Journal of Radiation Biology*, **37**, 207-212.
- Frankenberg-Schwager M., Frankenberg D., Blöcher D., Adamczyk C., 1979, The influence of oxygen on the survival and yield of DNA double-strand breaks in irradiated yeast cells. *International Journal of Radiation Biology*, No. **36**, N° 3, 261-270.
- Fuciarelli A. F., Wegher B. J., Blakely W. F. and Dizdaroglu M., 1990, Yields of radiation-induced base products in DNA: effects of DNA conformation and gassing conditions. *International Journal of Radiation Biology*, **58**, 397-415.
- Gomer R., 1975, *Interactions on Metal Surfaces*, Springer-Verlag, Berlin.
- Goodhead D. T., 1990, Models to link DNA damage to RBEs for final cellular effects. In *The early Effects of Radiation on DNA*, edited by Fielden M. and O'Neil P. (London: Springer).
- Goodhead D. T., 1994, Initial events in the cellular effects of ionizing radiations: clustered damage in DNA. *International Journal of Radiation Biology*, **65**, 7-17.
- Goodhead D. T., and Nikjoo H., 1990, Current status of ultrasoft x-rays and track structure analysis as tools for testing and developing biophysical models of radiation action. *Radiation. Protection Dosimetry* **31**, pp. 343-50.
- Hieda K., 1994, DNA damage induced by vacuum and soft X-ray photons from synchrotron radiation. *International Journal of Radiation Biology*, **66** (5), 561-567.

- Huels M. A., Hahndorf I., Illenberger E. and Sanche L., 1998, Resonant dissociation of DNA bases by subionization electrons. *Journal of Chemical Physics*, **108** (4), 1309–1312.
- Huels M. A., Khoury J., Boudaïffa B., Dugal P. C., Hunting D., Sanche L. and Waker A. J., 1996, A novel apparatus for low energy electron (0 - 5000 eV) irradiation of lyophilised DNA in an ultra-clean UHV environment, 12<sup>th</sup> Symposium on Microdosimetry, Sept. 29-Oct. 4, Oxford, U.K.
- Hutchinson F., 1954, Energy requirements for the inactivation of bovine serum albumin by radiation. *Radiation Research*, **1**, 43-52.
- Iskef H., Cunningham J. W. and Watt E. D., 1983, Projected ranges and effective stopping powers of electrons with energy between 20 eV and 10 KeV. *Physical Medical Biology*, **28**, 535-545.
- Ito T., Baker S.C., Stickley C.D., Peak J.G. and Peak M.J., 1993, Dependence of the yield of strand breaks induced by  $\gamma$ -rays in DNA on the physical conditions of exposure: water content and temperature. *International Journal of Radiation Biology*, **63**, 289-296.
- Kampf G., Tolkendorf E., Regel K., Abel H., 1977, Cell inactivation and DNA strand break rates irradiation with X-rays and fast neutrons. *Studia Biophysica*, **62**, S. 17-24.
- Kelbur J. A. and Knotek M. L., 1982, *Surface Science*, **121**, L499-L502.
- Kimmel G. A., Tonkyn R. G., Orlando T. M., 1995, *Nuclear Instruments & Methods B*, **101**, 179-183.

- Kimura M., Inokuti M., and Dillon M.A., 1993, Electron degradation in molecular substances. In *Advances in Chemical Physics*, edited by I. Prigogine and S.A. Rice (John Wiley & Sons, Inc.) p. 193.
- Krisch R. E., Flick M. B. and Trumbore C. N., 1991, Radiation chemical mechanisms of single- and double-strand break formation in irradiated SV40 DNA. *Radiation Research*, **126** (2), 251-259.
- LaVerne J. A., and Pimblott S. M., 1995, Electron energy-loss distributions in solid, dry DNA. *Radiation Research*, **141**, 208-215.
- Leclerc G., Zuolin C. and Sanche L., 1987, Effective dissociation cross section for low-energy electron impact on solid n-hexane thin films, *Journal of Physical Chemistry*, **91**, 6461-6466.
- Lehmann A. R., and Ormerod M. G., 1970, Double-strand breaks in the DNA of a mammalian cell after X-irradiation. *Biochimica et Biophysica ACTA*, **217**, 268-277.
- Maniatis T., Fritsch E. F., Sambrook J., 1982, *Molecular Cloning. A Laboratory Manual*. Cold Spring Harbor Laboratory Press (Cold Spring Harbor, N.Y.).
- Marsolais R. M., Cartier E. A., Pfluger P., 1991, Hot electron transport in condensed organic dielectrics. In *Excess Electron in Dielectric Media*, edited by C. Ferradini and J.-P. Jay-Gerin (Boca Raton: CRC Press), pp. 43-74.
- Michael B. D., Prise K. M., Folkard M., Vojnovic B., Brocklehurst B., Munro I. H. and Hopkirk A., 1994, Action spectra for single and double strand break induction in plasmid DNA: studies using synchrotron radiation. *International Journal of Radiation Biology*, **66** (5), 569-572.

- Michalik V. and Frankenberg D., 1994, Simple and complex double-strand breaks induced by electrons. *International Journal of Radiation Biology*, **66** (5), 467-470.
- Michalik V. and Frankenberg D., 1996, Two types of double-strand breaks in electron and photon tracks and their relation to exchange-type chromosome aberrations. *Radiation Environment Biophysics*, **35**, 163-169.
- Michaud M. and Sanche L., 1987, Absolute vibrational excitation cross sections for slow electrons (1-18 eV) scattering in solid H<sub>2</sub>O. *Physical Review A* **36**, 4684-46...
- Michaud M. and Sanche L., 1999, Absolute inelastic cross sections for 1-100 eV electrons scattering in amorphous H<sub>2</sub>O (in preparation).
- Michalik V., 1993, Energy deposition clusters in nanometer regions of charged particle track. *Radiation Research*, **134**, 265-270.
- Milligan J. R., Aguilera J. A. and Ward J. F., 1993, Variation of single-strand break yield with scavenger concentration for plasmid DNA irradiated in aqueous solution. *Radiation Research*, **113**, 151-157.
- Nikjoo H. and Goodhead D. T., 1991, Track structure analysis illustrating the prominent role of low-energy electrons in radiobiological effects of low-LET radiations, *Physics in Medicine and Biology*, **36**, N° 2, 229-238.
- Nikjoo H., and Goodhead D. T., 1989, The relative effectiveness (RBE) achievable by high and low LET radiations. *Low Dose Radiation* ed. K. Baverstock and J. Stather (London: Taylor & Francis), pp. 491-502.

- Nikjoo H., Goodhead D. T., Charlton D. E. and Paretzke H. G., 1991, Energy deposition in small cylindrical targets by monoenergetic electrons. *International Journal of Radiation Biology*, **60** (5), 739-756.
- Paretzke H. G., 1987, Radiation track structure theory. In *Kinetics of Nonhomogeneous Processes*, edited by G.R. Freeman (New York: Wiley), pp. 89-170.
- Paretzke H. G., Goodhead D. T., Kaplan I. G., and Terrissol M., 1995, Track structure quantities. In *Atomic and Molecular Data for Radiotherapy and Radiation Research*. TECDOC-799, IAEA, Vienna, pp. 633-721.
- Pimblott S. M., and LaVerne J. A., 1995, Energy loss by electrons in DNA. In *Radiation Damage in DNA: Structure/Function Relationships at Early Times*, edited by A. F. Fuciarelli and J. D. Zimbrick (Battelle Press), pp. 3-12.
- Pimblott S.M., LaVerne J.A., and Mozumder A., 1996, Monte Carlo simulation of range and energy deposition by electrons in gaseous and liquid water, *Journal of Physical Chemistry* **100**, 8595-8606.
- Platzman R. L., 1955, *Radiation Research*, **2**, 1.
- Prise K. M., Davies S. and Michael B. D., 1993, Evidence for induction of DNA double-strand breaks at paired radical sites. *Radiation Research*, **134** (1), 102-106.
- Rowntree P., Parenteau L. and Sanche L., 1991a, *Journal of Physical Chemistry*, **95**, 523.
- Rowntree P., Parenteau L. and Sanche L., 1991b, *Journal of Physical Chemistry*, **95**, 4903.

- Sanche L., 1991, Primary interactions of low energy electrons in condensed matter, In *Excess Electrons in Dielectric Media*, edited by C. Ferradini and J. P. Jay-Gerin (Boca Raton: CRC Press, Inc.), pp. 1-42.
- Sanche L., 1995, Interactions of low-energy electrons with atomic and molecular solids. *Scanning Microscopy*, **9**, 619-656.
- Sanche L., 1997, Nanoscopic aspects of electronic aging in dielectrics. In *IEEE Transaction on Dielectrics and Electrical Insulation*, **4**, 507-543.
- Siddiqi M. A. and Bothe E., 1987, Single and double-strand break formation in DNA irradiated in aqueous solution: dependence on dose and OH radical scavenger concentration. *Radiation Research*, **112** (3), 449-463.
- Siddiqi M. A., and Bothe E., 1987, Single- and double-strand formation in DNA irradiated in aqueous solution : dependence on dose and OH radical scavenger concentration. *Radiation Research*, **112**, 449-463.
- Spothem-Maurizot M., Charlier M., and Sabattier R., 1990, DNA radiolysis by fast neutrons, *International Journal of Radiation Biology*, **57**, n° 2, 301-313.
- Swarts, S. G., Sevilla, M. D., Becker, D., Tokar, C. J. and Wheeler, K. T., 1992, Radiation-induced DNA damage as a function of hydration 1. Release of unaltered bases. *Radiation Research*, **129**, 333-344.
- Tougaard S. and Chorkendorff I., 1987, Differential inelastic electron scattering cross sections from experimental reflection electron-energy-loss spectra. *Physical Review B* **35**, 6570.



- Uehara S. and Nikjoo H., 1996, Energy spectra of secondary electrons in water vapour. *Radiation and Environmental Biophysics*, **35**, 153-157.
- Vologodskii, A., 1992, Topology and physics of circular DNA (CRC Press, Inc.).
- von Sonntag C., *The Chemical Basis for Radiation Biology* (Taylor and Francis, London, 1987).
- Ward J. F., 1981, Some biochemical consequences of the spatial distribution of ionizing radiation-produced free radicals. *Radiation Research*, **86** (2), 185-195.
- Ward J. F., 1985, Biochemistry of DNA lesions. *Radiation Research*, **104**, S103-S111.
- Zimmerer G., 1987 in *Excited-State Spectroscopy in Solids*, edited by Grassano U. M. and Terzu N., North Holland, Amsterdam.

***III.2. ARTICLE N° 2: Resonant formation of DNA strand breaks by low energy (3 -- 20 eV) electrons. Science, Vol 287, p. 1658-1660 (2000).***

## **Resonant Formation of DNA Strand Breaks by Low Energy (3 – 20 eV) Electrons**

**Badia Boudaïffa, Pierre Cloutier, Darel Hunting, Michael A. Huels, Léon Sanche**

Canadian Medical Research Council Group in Radiation Sciences, Department of Nuclear Medicine and Radibiology, Faculty of Medicine, University of Sherbrooke, Québec, Canada J1H 5N4

**Most of the energy deposited in cells by ionizing radiation is channeled into production of abundant free secondary-electrons with ballistic energies between 1 and 20 eV. Here it is shown that reactions of such electrons, even at energies well below ionization thresholds, induce significant yields of single and double strand breaks in DNA, which are caused by rapid decays of transient molecular resonances localized on the DNA's basic components. This fundamentally challenges the traditional notion that genotoxic damage by secondary-electrons can only occur at energies above the onset of ionization, or upon solvation when they become a slowly reacting chemical species.**

The genotoxic effects of ionizing radiations ( $\beta$ , X, or  $\gamma$ -rays) in living cells are not produced by the mere direct impact of the primary high energy quanta. Instead, mutagenic, recombinogenic, and other potentially lethal DNA lesions (1 - 3), such as single and double strand breaks (SSB, DSB) are induced by secondary species generated

by the primary ionizing radiation (4). Free secondary electrons, with energies between about 1 and 20 eV, are the most abundant ( $\approx 5 \times 10^4/\text{MeV}$ ) of these secondary species (5 - 8), but it is unclear if such low energy electrons are able to induce genotoxic damage, such as SSB or DSB (9). In order to investigate this, we have irradiated plasmid DNA with a very low energy electron (LEE) source under ultra-high-vacuum (UHV) conditions, since condensed phase electron-molecule interactions are highly sensitive to minor impurities (10, 11). Our previous work on small bio-organic molecules (12 - 15) allowed us to develop and adapt the necessary electron microbeam techniques to determine the effects of very low energy, non-thermal secondary electrons on the entire DNA molecule at various well defined incident electron energies between 3 and 20 eV. The experiments were performed at  $10^{-9}$  Torr in a hydrocarbon-free environment, and all sample manipulation occurred in a sealed glove box under a pure dry nitrogen atmosphere.

Plasmid DNA (pGEM 3Zf(-), 3199 bp) was extracted from *E. coli* DH5 $\alpha$ , purified and resuspended in nano-pure water (without any Tris or EDTA). An aliquot of this pure aqueous DNA solution was deposited onto chemically clean Tantalum substrates held at liquid nitrogen temperatures, lyophilized with a hydrocarbon-free sorption pump at 5 mTorr (16), and transferred directly to the UHV chamber without exposure to air or further characterization. After evacuation ( $\approx 24$  hrs), the room temperature DNA solids were irradiated with a monochromatic LEE beam for a specific time at a fixed beam current-density ( $2.2 \times 10^{12}$  electrons  $\text{s}^{-1} \text{cm}^{-2}$ ) and incident electron energy. Thus, the LEE irradiations are performed on clean DNA, containing its structural water (17). DNA was then analyzed by agarose gel electrophoresis, and quantified as supercoiled (SC,

undamaged), nicked circle (SSB), full length linear (DSB), and short linear forms; the first three species produce well resolved bands and the latter produce a smear.

The measured DNA damage yields (Fig. 1) show three striking characteristics: First, very low energy electron irradiation can induce significant damage in DNA, namely SSB and DSB, even at electron energies well below the DNA's ionization limit (7.5 – 10 eV) (18); Second, DNA damage by 3 - 20 eV electrons is highly dependent on the initial kinetic energy of the incident electron, particularly below 14 - 15 eV where we observed thresholds near 3 - 5 eV and intense peaks near 10 eV. This is in sharp contrast to DNA strand breaks induced by similarly energetic photons, where both SSBs and DSBs have been found to increase monotonically above a threshold near 7 eV and remain relatively constant above circa 12 eV (19), up to about 2 keV (20). Third, the SSB and DSB peak yield values measured here above 7 eV ( $8.2 \times 10^{-4}$  and  $2 \times 10^{-4}$  strand breaks per incident electron, respectively, at the 10 eV peak) are roughly one to two orders of magnitude larger than those for 10 - 25 eV photons (20). For 7 - 25 eV photons, the ratio of SSB to DSB is about 30 : 1, whereas for 7 - 20 eV electrons it is about 4 : 1 on average. Thus, the mechanisms of DNA damage depend not only on the quantum of energy absorbed, but also on the nature of the particle that deposits the energy.

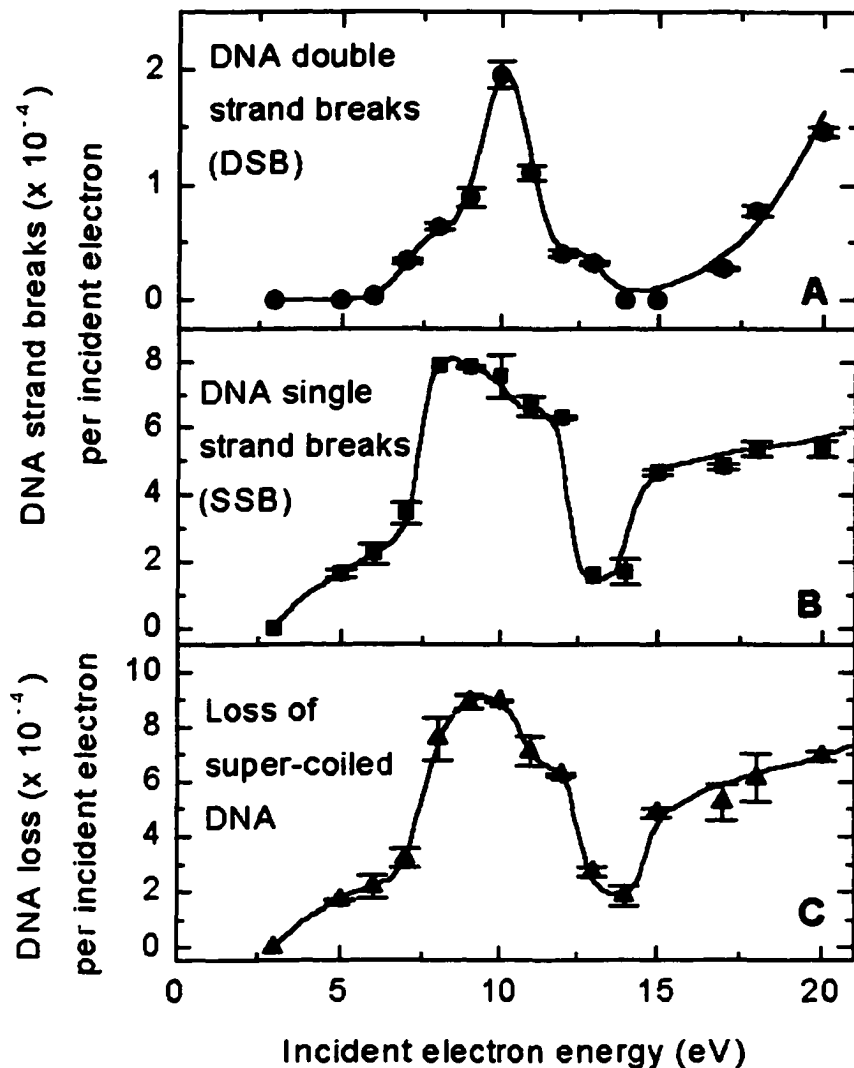


**Fig. 1:** Measured quantum yields, solid symbols (per incident electron), for the induction of DSB (A), SSB (B), and loss of the supercoiled (SC) DNA form (C), in DNA solids by low energy electron irradiation, as a function of incident electron energy; the solid curves are guides to the eye. High purity DNA solids were irradiated under UHV with an electron beam at various incident energies and electron exposures (exposure = time of irradiation  $\times$  current-density  $\times$  target area), with an energy resolution of 0.5 eV. A Faraday detector slit (0.3 mm wide) as well as phosphorescent plates were used to verify optimum spatial overlap between the the DNA solid (circa 6 mm diameter) and the incident electron beam, which is collimated onto the target area via an *in vacuo* coaxial electromagnetic coil (20 Gauß). After electron irradiation, the DNA was dissolved in

buffer (Tris-EDTA: 10 mM/1 mM; pH 7.5), and analyzed by agarose gel electrophoresis. Gels were stained with SYBR Green I solution (1:10,000; Molecular Probes, Eugene OR) and scanned by laser (Storm, Molecular Dynamics, Sunnyvale CA). Quantitative analysis of DNA damage was performed using the ImageQuant program (Molecular Dynamics). Damage yields were determined from linear least square fits to the initial slopes of the incident-electron exposure-response curves (in the very low exposure, linear response regime), at each incident electron energy, for SC DNA loss and production of nicked circle (SSB) and full length linear (DSB) forms (29). Each data point corresponds to an average of about five independent exposure-response slope measurements (each consisting of 8 - 12 DNA samples, irradiated with electrons at increasing exposures). The error bars correspond to one standard deviation of the average slope, or reproducibility, of the measurement. Comparison of control samples held in solution, with unirradiated samples held under UHV conditions for equal time periods, showed that deposition and recovery of plasmid DNA introduces only small amounts of SSB (5 - 10% on the average) and no detectable DSB.

The strong electron energy dependence of the DNA strand breaks, observed here below 14 eV, is attributed to electron attachment somewhere within the DNA molecule, followed by localized bond rupture, and subsequent reactions of the fragmentation products. Electron attachment (21) is best illustrated by the type of damage it induces in thin films consisting of very small molecules, such as thymine (13), H<sub>2</sub>O (22), or a deoxyribose analogue (14), summarized in Fig. 2. These and other electron impact experiments (15), including some on small linear (23, 24) and cyclic (11, 12, 25) hydrocarbons, have shown that electrons with energies below 15 eV initiate fragmentation of small molecules essentially by attachment of the incident electron; this leads to the formation of a resonance, namely a transient molecular anion (TMA) state. For a molecule RH this corresponds to:  $e^- + RH \rightarrow RH^{*-}$ , where the  $RH^{*-}$  has a repulsive potential along the R-H bond coordinate. This TMA can decay via electron autodetachment (26) or by dissociation along one, or several (12, 14, 25), specific bonds such as  $RH^{*-} \rightarrow R^* + H^-$ .

The probability for attachment and subsequent decay via either channel is in part defined by the repulsiveness of the  $RH^{*-}$  potential energy surface and its uncertainty energy width  $\Gamma = \hbar/\tau$ , where  $\tau$  is the electron autodetachment lifetime (typically  $10^{-14}$  to  $10^{-13}$  s) of the TMA as given by the Heisenberg uncertainty principle. In quantum terms, electron attachment is allowed via a vertical electronic transition to the state  $RH^{*-}$  only at energies for which there is sufficient overlap between the nuclear wave-functions of the initial ground state neutral and final anion states. This corresponds conceptually to a reflection of the RH ground state wavefunction (of Gaussian shape) by the repulsive curve  $RH^{*-}$ , and results in the peaks in the anion fragment yields shown in Fig. 2.



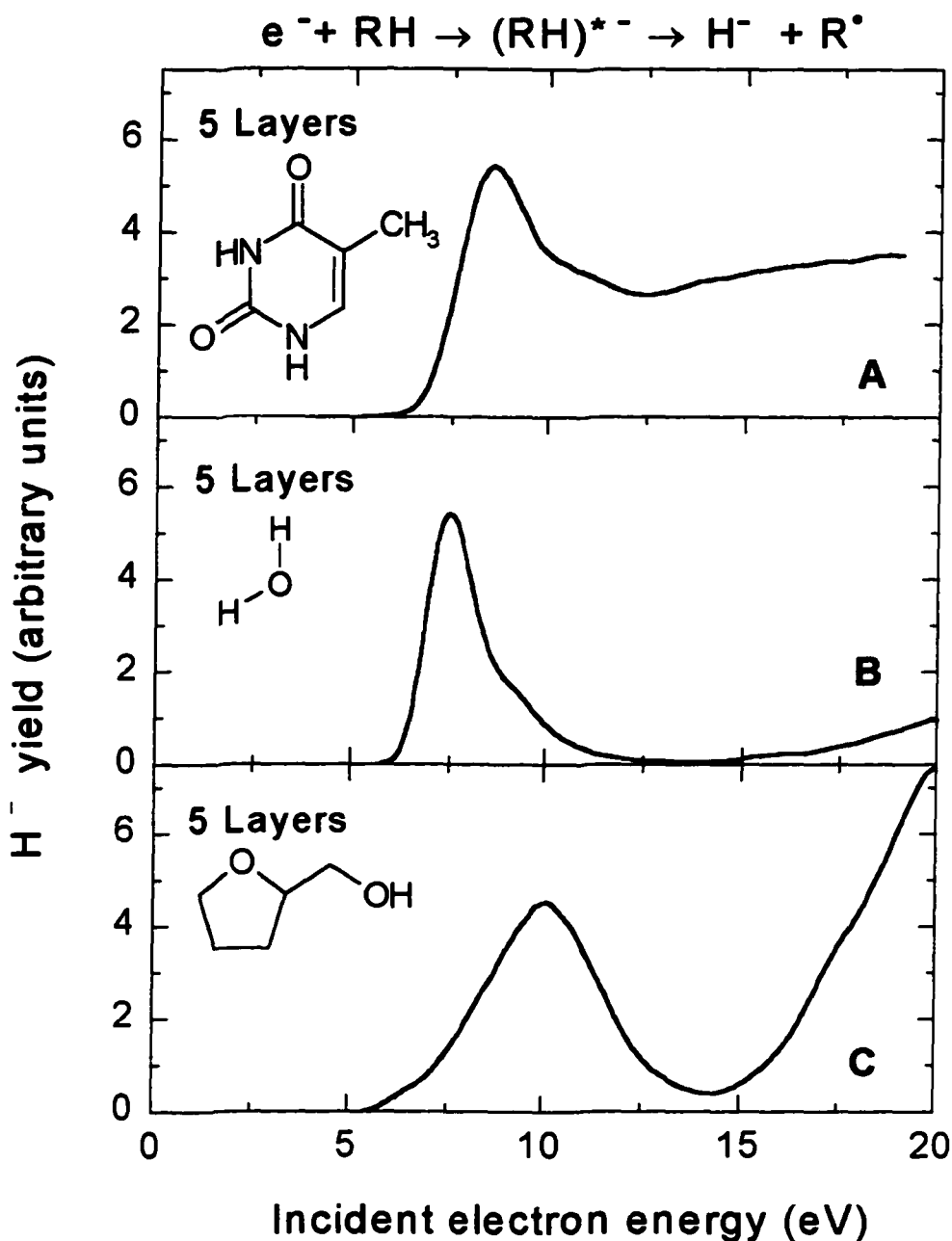


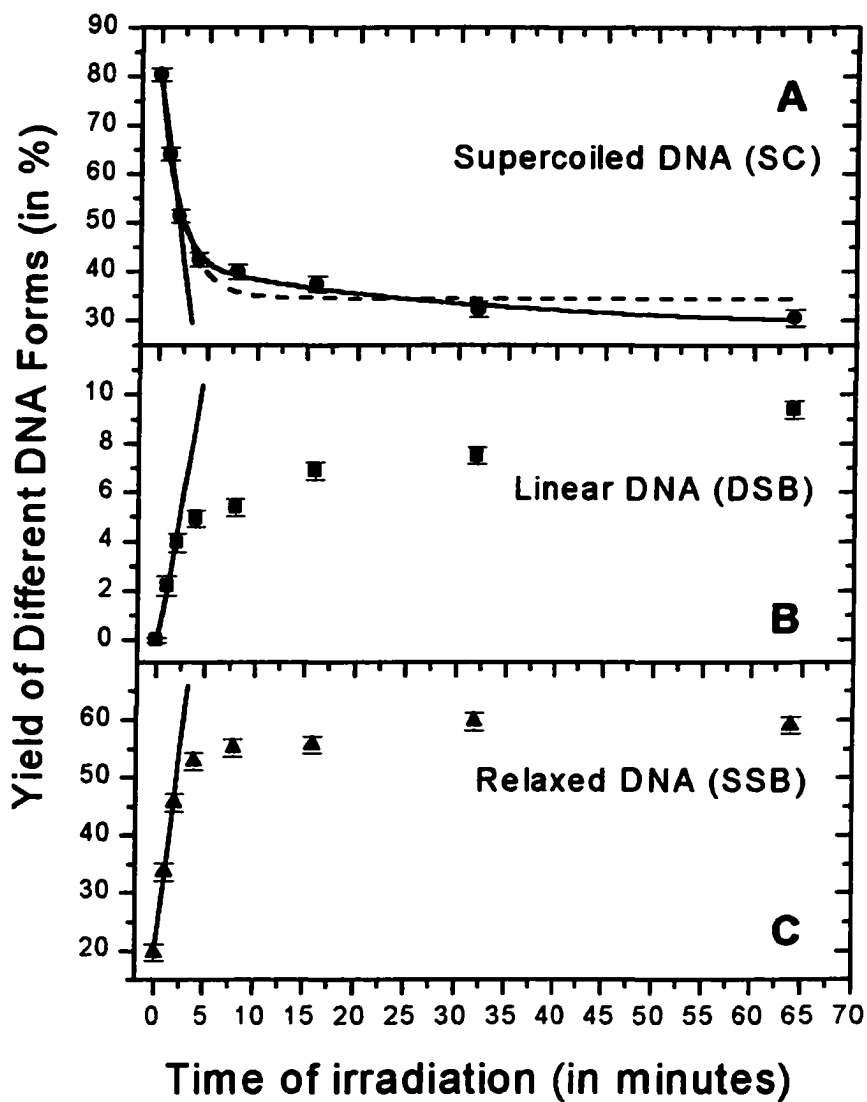
**Fig. 2:** Electron damage to condensed films of molecules  $RH$  = thymine (A), water (B), and tetrahydro-furfuryl alcohol (C), exemplified in the form of electron energy dependent desorption yields of energetic  $H^-$  (1 - 4 eV). These and other fragments emanate from the thin films during electron impact, due to formation and subsequent dissociation of electron-molecule resonances  $RH^{\bullet -}$ . Each film is circa five monolayers thick, and is prepared and irradiated under UHV conditions ( $10^{-10}$  Torr). The experimental methods are discussed elsewhere (14, 22).

The branching ratio between electron autodetachment and bond dissociation depends in part on the above intrinsic characteristics of the specific TMA, whereas the final damage yields also depend on extrinsic effects (10) such as electron energy losses, or fragment reactions, any of which depend on the structural and chemical composition of the immediate molecular environment. The latter will thus modify the resonant response of the pure individual components of DNA (Fig. 2) when localized within a DNA double strand (Fig. 1). Non-resonant electronic excitations to neutral states  $RH^*$  may also lead to bond cleavage, and are allowed at any energy above a threshold, thus contributing a monotonically rising signal to the final anion yields in Fig. 2 above circa 12 - 13 eV.

Thus, based on the present measurements and relative dimensions of the various DNA components and the quantum size of the incident electron, we conclude that the observed DNA strand breaks (Fig. 1 below 14 eV) are initiated by resonant electron attachment to the various basic DNA components (base, deoxyribose, phosphate, or hydration  $H_2O$ ), followed by bond dissociations within the TMA's lifetime, usually femtoseconds. Whereas this event itself may already generate a SSB, the observation of DSB at incident electron energies well below those required for two ionizations ( $> 20$  eV) within 10 bp of each other on opposing phosphate-sugar strands (19), suggests that some fragmentation products subsequently react locally with other DNA components, and lead to a doubly damaged site with breaks on opposing strands. This is supported by the observation of electron initiated fragment reactions (such as hydrogen abstraction, dissociative charge transfer, atom and functional group exchange, and reactive scattering) occurring over distances comparable to the DNA's double strand diameter (circa 1 - 2 nm) in condensed films containing water (27) or small linear and cyclic hydrocarbons

(11, 24). The 5.5 – 6 eV shoulder observed in the SSB yield curve (but not the DSB yield curve) is possibly related to various electron induced fragmentation channels observed in gas phase cytosine and thymine below 10 eV (12) (or equivalent fragmentations in adenine or guanine).

Our results suggest that the abundant low energy (1 - 20 eV) secondary-electrons, and most likely their ionic and radical reaction products, play a crucial role in the nascent stages of DNA radiolysis, and may already induce significant damage long before their thermalization, or the diffusion limited reactions of other secondary species produced along ionizing radiation tracks. Since the resonant electron-molecule interactions, observed here, occur in small molecules regardless of their aggregation state (28), they are expected to be operative in living cells as well. It is only through a complete understanding of such early events in the generation of genotoxic damage that we may hope to eventually manipulate the effects of ionizing radiation at a molecular level.



**Supplemental figure 1.** Exposure- response at 11 eV incident electron energy, for the loss of supercoiled DNA and production of SSB and DSB DNA forms. The dashed curve in (A) is a first-order exponential fit to the SC data, and the solid curve is a second-order exponential fit..

**References:**

1. J. F. Ward, in *Advances in Radiation Biology* 5. J.T Lett, and H. Adler, Eds. (Academic, New York, 1977) pp. 181 - 239.
2. O. Yamamoto, in *Aging, Carcinogenesis and Radiation Biology*. K. Smith, Ed. (Plenum, New York, 1976) pp. 165 - 192.
3. A. F. Fuciarelli and J. D. Zimbrick, Eds., *Radiation Damage in DNA: Structure/Function Relationships at Early Times*. (Battelle, Columbus, OH, 1995).
4. C. von Sonntag, *The Chemical Basis for Radiation Biology* (Taylor and Francis, London, 1987).
5. *ICRU Report 31*, International Commission on Radiation Units and Measurements, Washington, DC (1979).
6. S. M. Pimblott and J. A. LaVerne, in (3), pp. 3 - 12.
7. V. Cobut *et al.*, *Radiat. Phys. Chem.* **51**, 229 (1998).
8. D. Srdoc *et al.*, in *IAEA CRP Atomic and Molecular Data for Radiotherapy and Radiation Research*. M. Inokuti, Ed. (IAEA press, Vienna, 1995) chapter 8.
9. The only previous low energy work concentrated on DNA damage by 25 - 4000 eV electrons, see M. Folkard, K. M. Prise, B. Vojnovic, S. Davies, M. J. Roper, B. D. Michael, *Int. J. Radiat. Biol.*, **64**, 651 (1993). In that study the samples were exposed to high background gas pressures ( $10^{-5}$  -  $10^{-6}$  torr), and contained salt (EDTA, ratio of DNA-to-EDTA = 1 : 1 by weight) during electron irradiation; the latter was reported to shield the DNA towards low energy electrons.
10. M. A. Huels, L. Parenteau, L. Sanche, *J. Chem. Phys.*, **100**, 3940 (1994).
11. M. A. Huels, L. Parenteau, L. Sanche, *Chem. Phys. Lett.* **279**, 223 (1997).

12. M. A. Huels, I. Hahndorf, E. Illenberger, L. Sanche, *J. Chem. Phys.* **108**, 1309 (1998).
13. L. Sanche, unpublished.
14. D. Antic, L. Parenteau, M. Lepage, L. Sanche, *J. Phys. Chem.* **103**, 6611 (1999).
15. For a review see: A. D. Bass and L. Sanche, *Radiat. Environ. Biophys.* **37**, 243 (1998).
16. Each sample consisted of 500 ng of purified DNA in 10  $\mu$ L of nanopure water, which was deposited on a Tantalum substrate over a measured area of about 6 mm average diameter. After lyophilization, this results in a pure solid calculated to be of 10 nm average thickness at a known density of 1.7 g cm<sup>-3</sup>, assuming minimal clustering of the plasmids in the solid.
17. Desiccation leaves plasmid DNA with its structural water of about 2.5 water molecules per base pair (S. G. Swarts, M. D. Sevilla, D. Becker, C. J. Tokar, K. T. Wheeler, *Radiat. Res.* **129**, 333 (1992)), with the plasmid solids containing a mixture of A and C conformations. Removal of this intrinsic hydration water is believed to lead to substantial conformational changes and double strand breaks, which is not observed in our unirradiated control samples held under UHV.
18. A. O. Colson, B. Besler, M. D. Sevilla, *J. Phys. Chem.* **96**, 9787 (1992).
19. K. Hieda, *Int. J. Radiat. Biol.* **66**, 561 (1994).
20. B. D. Michael *et al.*, in (3), pp. 251 - 258.
21. For a review see: L. Sanche, *Scanning Microsc.* **9**, 619 (1995).
22. P. Rowntree, L. Parenteau, L. Sanche, *J. Chem. Phys.* **94**, 8570 (1991)
23. P. Rowntree, L. Parenteau, L. Sanche, *J. Phys. Chem.* **95**, 4902 (1991).
24. A. D. Bass, L. Parenteau, M. A. Huels, L. Sanche, *J. Chem. Phys.* **109**, 8635 (1998).

25. M. Stepanovic, Y. Pariat, M. Allan, *J. Chem. Phys.* **110**, 11376 (1999).
26. For vertical electron attachment energies in gas phase nucleobases below 5 eV see K. Aflatooni, G. A. Gallup, P. D. Burrow, *J. Phys. Chem.* **A102**, 6205 (1998); for detachment energies in solvated uracil cluster anions see J. H. Hendricks, S. A. Lyapustina, H. L. de Clercq, K. H. Bowen, *J. Chem. Phys.* **108**, 8 (1998).
27. M.T. Sieger, W. C. Simpson, T. M. Orlando, *Nature* **394**, 554 (1998).
28. L. G. Christophorou, E. Illenberger, W. Schmidt, Eds. *Linking the Gaseous and Condensed Phases of Matter: the Behaviour of Slow Electrons*. Nato ASI Series B: physics Vol. **326** (Plenum, NY, 1994).
29. Sample exposure-response curves (Supplemental figure 1.) can be seen at Science online ([www.sciencemag.org/feature/data/1044957.sh1](http://www.sciencemag.org/feature/data/1044957.sh1)).
30. We thank A. J. Waker for helpful comments and suggestions. Supported by the Medical Research Council of Canada, and the Atomic Energy of Canada Ltd.

***III.3. ARTICLE N° 3 : DNA Damage Induced by Low-Energy (3 – 100 eV) Electrons***



## **DNA DAMAGE INDUCED by LOW ENERGY (3 – 100 eV) ELECTRONS**

*Badia Boudaïffa et al.*

Canadian Medical Research Council Group in the Radiation Sciences, Dept. of Nuclear Medicine and Radiobiology, Faculty of Medicine, University of Sherbrooke, Québec, Canada J1H 5N4;

**We report measurements of low-energy (3-100 eV) electrons impact on plasmid DNA. Electron bombardment to DNA induce single, double and multiple strand breaks. We show that significant damage occurs with very low energy deposition (< 15 eV) induced mainly by the formation of dissociative electron attachment (DEA) via resonance mechanisms. However with higher energy (> 15 eV), multiple electron scattering is believed to contribute to the increase of strand breaks. Non-resonant mechanisms, such as dipolar dissociation, single and double ionization may be responsible for DNA damage. Our results demonstrate that secondary electrons contribute significantly to biological damage prior to their solvation, via resonant mechanisms by a similar intensity than those produced via non-resonant mechanisms.**

Many of the mutagenic or lethal effects of ionizing radiation can be traced to structural and chemical modifications of cellular DNA.<sup>1, 2, 3</sup> This damage may take the form of, e.g., single strand break (SSB) and double strand break (DSB),<sup>1</sup> base and sugar modifications,<sup>4</sup> or DNA-protein cross links;<sup>2</sup> it is therefore crucial to understand the various mechanisms that lead to a final biological outcome. Studies on DNA are usually

concentrated on the damage induced either by the initial irradiation, e.g. very energetic primary or secondary electrons (MeV to KeV range), or by slow, viz. diffusion controlled, reactions of thermal cations, radicals, or solvated / hydrated electrons produced along their tracks. However, the vast majority of secondary electrons produced along radiation tracks have initial kinetic energies well below 100 eV but well above thermal energies (unsolvated or hyperthermal). Since these secondary electrons are solvated within  $10^{-12}$  s after the initial ionizing event via successive inelastic collisions within the biological medium, they may induce DNA damage within femto-second timescales; thus the DNA strand is likely to be already damaged prior to the beginning of diffusion limited reactions initiated by other secondary reactive species.

Our present measurements of electron induced single, double, and multiple strand breaks (MSB) show that secondary electron induced events include those that lead to significant strand lesions, and are associated with localized fragmentations of the various constituent components of DNA by low energy electrons.

Our previous work on small bio-organic molecules<sup>5, 6, 7, 8</sup> has allowed us to develop and adapt the necessary ultra-high vacuum (UHV) electron microbeam techniques to standard biological methods to probe the damaging effects of low-energy electrons on DNA itself. The experimental techniques are discussed in detail elsewhere<sup>9, 10</sup>, and only a brief description is given here.

In order to yield reliable results, the present measurements employ UHV methods and all sample preparation and manipulation is carried out within a sealed glove box under a pure dry nitrogen atmosphere. An aliquot of nano-pure aqueous DNA solution (pGEM 3Zf(-), 3199 bp) exempt of salt and other molecular contaminants is deposited onto

chemically clean tantalum (Ta) substrates. The samples are lyophilized with a hydrocarbon-free sorption pump at 5 mTorr and transferred from the glove box directly to the UHV irradiation chamber without exposure to air. In the UHV chamber the DNA films are irradiated with a monochromatic electron beam. After irradiation, the DNA is dissolved in buffer (Tris-EDTA: 10 mM/1 mM; pH 7.5) and analysed by agarose gel electrophoresis. The gels are scanned by laser using a Storm (Molecular dynamics) and quantitative analysis of DNA damage, corresponding to supercoiled, nicked circle, full length linear and short linear, is performed using ImageQuant program (Molecular dynamics).

The measured yields (events per incident electron) for the loss of the supercoiled (SC) form, and the induction of SSB, DSB and multiple strand breaks (MSB) in plasmid DNA by low energy electron (LEE) irradiation, as a function of incident electron energy (0-100 eV), are displayed in figure 1. The yields are determined from least square fits to the initial slopes of the incident electron flux-response curves, at each incident electron energy, for SC DNA loss and production of nicked circle, full length linear and short fragments DNA (i.e. in the very low flux region of 100 nA after 1 to 3 min of irradiation) as discussed previously <sup>10</sup>. Each data point corresponds to an average of about five independent flux-response slope measurements, and the error bars correspond to one standard deviation of that average. We distinguish between features appearing in the low incident-electron energy region, i.e., below 15 eV, and those appearing in the high incident-electron energy above this threshold. As this low-energy region has previously been studied <sup>9, 10</sup>, we only summarize those findings here. For  $E_i$  between 3 and 15 eV, the structure of the curves has a maximum signal intensity near an  $E_i$  of 10 eV, and has

been associated with the formation of dissociative electron attachment (DEA) via resonant mechanisms within the DNA molecule followed by localized bond rupture, and subsequent reactions of the fragmentation products<sup>9</sup>.

In the incident-electron-energy region between 14 and 20 eV, we observe a plateau in the induced SSB yield in favor of the induction of DSB which increase significantly up to 20 eV. SSB yield increases above 20 eV, reaching a maximum at 30 eV and remains constant up to 100 eV. In contrast, DSB yield continues to increase above 20 eV, but less steeply than below this threshold. DSB yield increases slowly above 40 eV while the yield of MSB increases rapidly compared to the yield below 40 eV.

This results show that very low energy electron irradiation can induce significant damage in DNA, namely SSB, DSB and MSB, even at electron energies well below the medium's ionization limit (8 – 10 eV)<sup>11</sup>; we note also that DNA damage by secondary electrons is highly sensitive to the initial kinetic energy of the electron, especially below 15 eV where resonant mechanisms of damage induction predominate. Indeed, electrons with energies below 15 eV are known to be resonant with small molecules leading to the temporary attachment of an incident electron in a usually unfilled orbital. When the transient molecular anion (TMA) thus formed is dissociative, fragmentation occurs. For a molecule RH this corresponds to:  $e^- + RH \rightarrow RH^{*-}$ , where the  $RH^{*-}$  has a repulsive potential along the R-H bond coordinate. This TMA can decay via electron autodetachment<sup>12</sup> or by dissociation along one, or several<sup>5, 7, 13</sup>, specific bonds such as  $RH^{*-} \rightarrow R^\bullet + H^-$ .

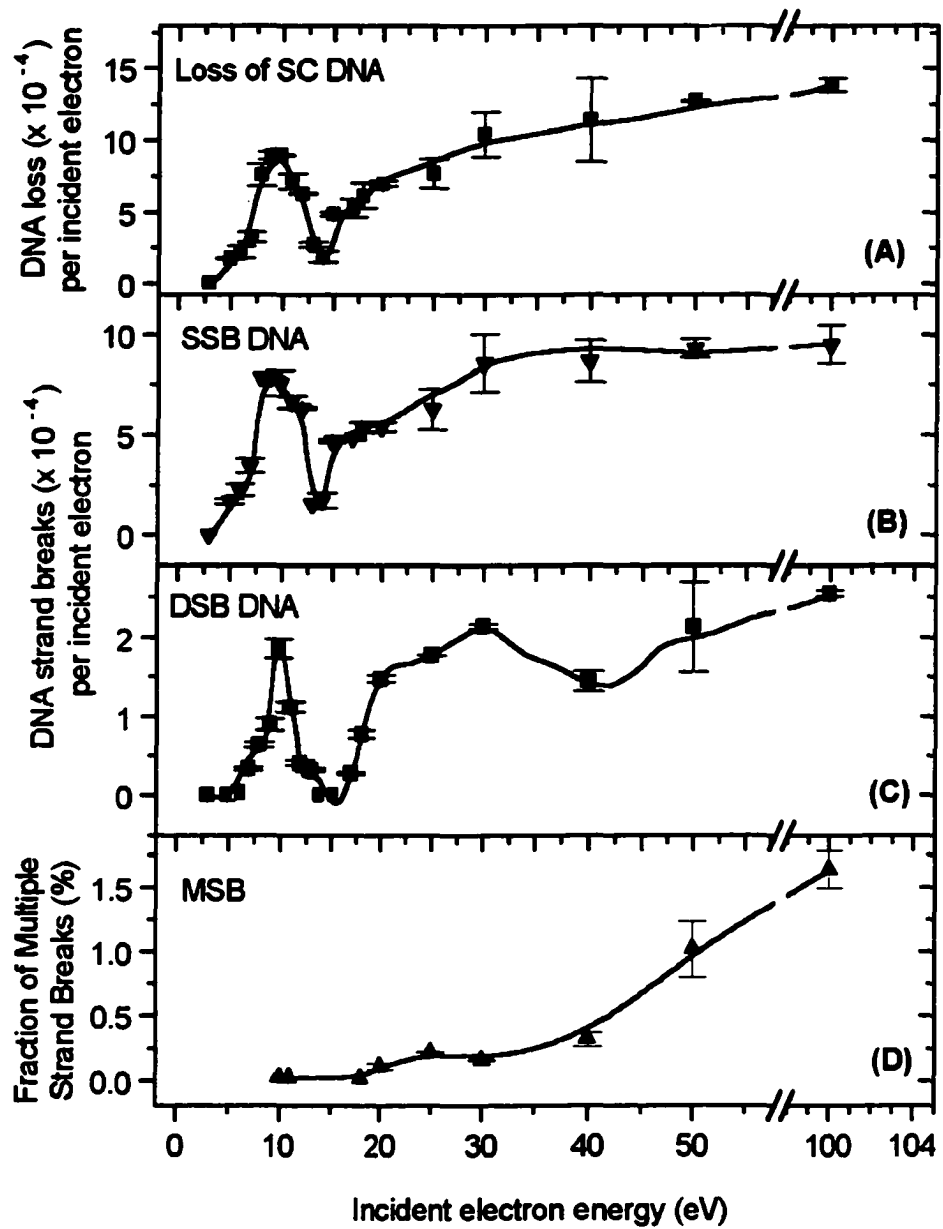


**Figure 1 :** Measured absolute total yields for loss of the supercoiled DNA form (A), and the induction of SSB (B), DSB (C) and MSB (D) in plasmid DNA as functions of incident electron energy.

The results show also that above this energy, the electron energy dependence, of the yields of SSB, and DSB usually increases monotonically. This is attributed to non-resonant mechanisms such as electronic transitions to excited states of the neutral molecule or its cations. Non-resonant electronic excitations to a neutral state  $(RH)^*$  may lead to bond cleavage via a number of different channels. The threshold energy for dissociation within the solid corresponds to the dissociation of the electronic state  $(RH)^*$  which can produce two radicals  $(R^\bullet + H^\bullet) + e^-$ .

At slightly higher energy ( $E > 15$  eV) isolated positive and negative species, screened by the polarization they induce in the solid, can be formed, e.g., dissociation into  $R^+$  and  $H^-$  fragments (dipolar dissociation, DD). This latter process usually produces a smooth continuous signal, which increases monotonically with electron energy. The released species can have kinetic energies ranging from meV's to a few eV's. It is therefore possible within 10-100 femtoseconds, for a radical created at one site of a given target to react at a another site located a few nm away, thus creating, e.g. within DNA a double strand breaks. This is qualitatively supported by LEE damage to gas and condensed phase bases<sup>14,15</sup> and thin films consisting of solid thymine and  $H_2O$ <sup>16</sup>. Analysis of these, and other electron impact experiments, including linear<sup>17,18</sup> and cyclic<sup>13</sup> hydrocarbons, and 6- and 12-mers of thymidine and cytidine monophosphate, has shown that for LEE above ca. 15 eV, non-resonant molecular fragmentation usually increase monotonically.

Single ionization (i.e.,  $[RH]^+ + e^-$ ) and multiple ionization ( $[RH]^{n+} + ne^-$ ) may also lead to bond cleavage, and are allowed at any energy above their respective thresholds. Thus they may also contribute along with the damages that can be created by the secondary electrons, to the monotonically rising signal in the yields shown in Fig. 1 above 15 eV. If

the positive ion  $(RH)^+$  is created in a dissociative state, a cation and a radical leave the molecular site with non-thermal energy. As explained previously, such species can react with their environment within a few nm and induce double and even multiple strand breaks. On the other hand, the secondary electrons produced by ionization can, depending on their energy, further ionize and dissociate molecules RH or temporarily attach to the molecule, forming a temporary state  $RH^-$  which can subsequently dissociate into the products  $R^- + H^+$  or  $R^+ + H^-$ , as discussed in the previous paragraph. Thus at energies above 15 eV multiple scattering becomes important and the density of radicals produced increases monotonically causing a similar increase in DNA strand breaks.

The formation of a particular MSB at these energies and at such low doses as shown in figure 2 for a fixed energy of 50 eV, may involve direct physical interactions of electrons with various DNA sites (sugar, bases,  $H_2O$ ) by a single event. We do not believe that multiple damage by multiple electron interactions occurs with present low-exposures. Indeed, short length linear DNA appears at relatively early times before substantial accumulation of linear form has occurred as seen with much lower energies (10-15 eV). This results indicate that at least a portion of MSB arise from multiple sites damage by a single electron. In general, this is possible if regions of the DNA which are distant in primary sequence along the DNA double strand are in close contact as discussed previously<sup>10</sup> (i.e. where the DNA helix crosses itself or is in close proximity to another part of the same DNA molecule). Thus, the deposition of sufficient energy in a small volume by low-energy electrons, could result in the formation of two DSB which are separated by hundreds of base pairs along the primary sequence.

The drastic increase in the yield of short fragments shows that the higher energy radiation is more efficient at producing MSB.

In conclusion, our present measurements of electron induced single, double, and multiple strand breaks (MSB) show that secondary electron induced events include those that lead to significant strand lesions, and are associated with localized fragmentations of the various constituent components of DNA by low energy electrons. We have demonstrated that the yield of SSB and DSB via a resonant electron mechanism at 10 eV is similar to that produced at 30-50 eV, where non-resonant mechanisms dominate including electronic excitation, dipolar dissociation and ionization, which cause multiple scattering with a production of high density of radicals. This has a particular relevance to the field of radiation science since it is well known that the majority of low-energy secondary electrons are produced along radiation tracks with initial kinetic energies well below about 20 eV. Thus, the damage induced by secondary electrons created in the hydration shell in the vicinity of DNA will be of significant relevance and the probability of DNA damage at  $E < 15$  eV will be more important and more dramatic than at  $E > 20$ -50 eV. Indeed, the recent results of Abdoul-Carime *et al.*, shows that the probability of damage by fragmentation induced 13 eV secondary electrons is about 3 times that found at 30 eV for oligonucleotides when the distribution of secondary electrons is taken into account<sup>19</sup>.



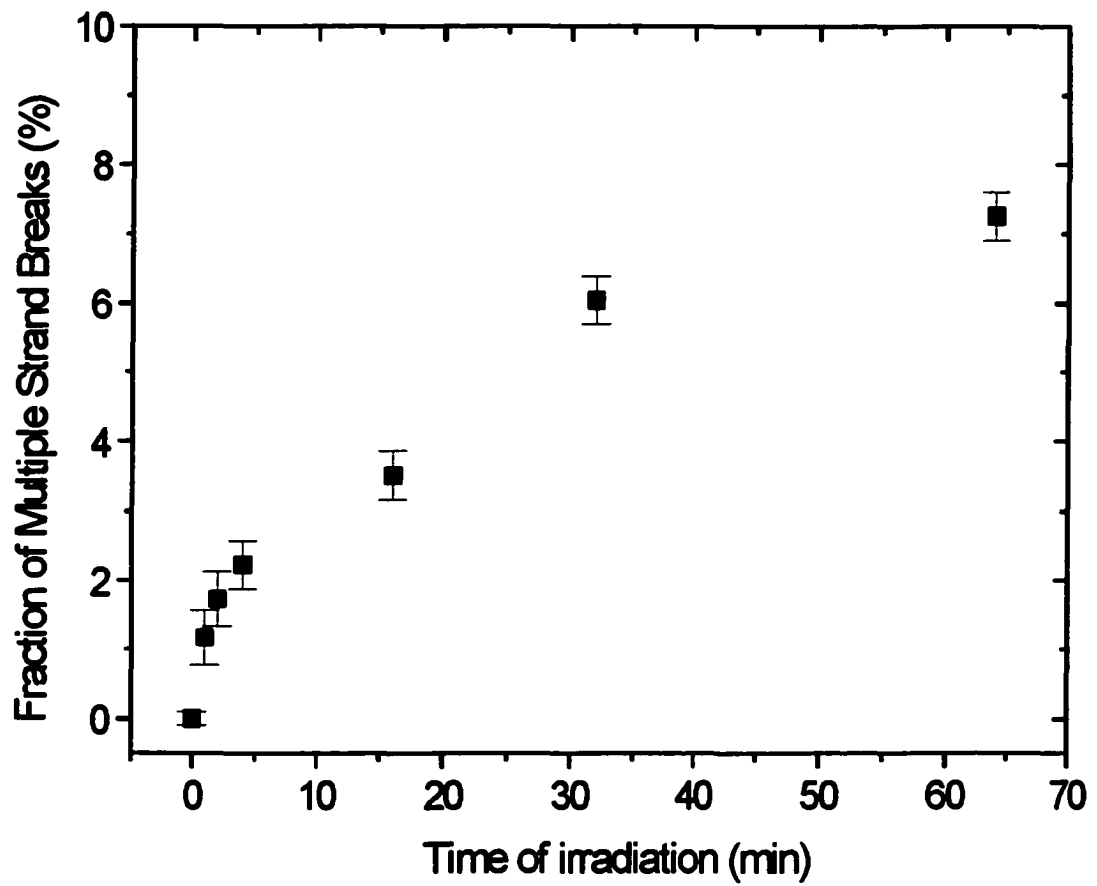


**Figure 2** : Exposure response at 50 eV incident electron energy for the induction of multiple strand breaks DNA (MSB).

## References

- <sup>1</sup> von Sonntag, C. *The chemical basis for radiation biology* (Taylor and Francis, London, 1987).
- <sup>2</sup> Yamamoto, O. In *Aging, Carcinogenesis and radiation biology*, ed. Smith, K. Plenum, New York, p. 165-192, (1976).
- <sup>3</sup> Radiation damage in DNA : *Structure/Function Relationships at Early Times*, edited by Fuciarelli, A. and Zimbrick, J. D. (Battelle, Columbus, Ohio, 1995)
- <sup>4</sup> Ward, J.F. In *Advances in radiation biology*, eds Lett, J.T. and Adler, H., Academic, New York, p. 181-239, (1972).
- <sup>5</sup> Huels, M.A.; Hahndorf, I.; Illenberger, E.; Sanche, L. Resonant dissociation of DNA bases by subionization electrons. *J. Chem. Phys.*, 108, 1309-1312, 1998.
- <sup>6</sup> Herve du Penhoat, M. A.; Cloutier, P.; Khoury, J.; Jay-Gerin, J. P.; Huels, M. A.; Sanche, L. to be published.
- <sup>7</sup> Antic, D., Parenteau, L., Lepage, M., Sanche, L., Low energy electron damage to condensed phase deoxyribose derivatives investigated by electron stimulated desorption of H<sup>-</sup> and electron energy loss spectroscopy. *J. Phys. Chem.* (1999) – in press.
- <sup>8</sup> Dugal, P. C.; Huels, M. A.; Sanche, L. Low-energy (5-25 eV) electron damage to homooligonucleotides, *Radiat. Res.*, 151, 325-333 (1999).
- <sup>9</sup> Boudaïffa B., Cloutier P., Hunting D., Huels M. A., and Sanche L., Resonant induction of DNA strand breaks by low energy (3 – 20 eV) electrons, *Science*, Vol 287, p. 1658-1660 (2000).
- <sup>10</sup> Boudaïffa B., Cloutier P., Hunting D., Huels M. A., Sanche L., Cross Sections for Low-Energy (3-50 eV) Electron Damage to DNA. In preparation.

- <sup>11</sup> Colson A. O., Besler B. and Sevilla M. D., Ab-initio orbital calculations on DNA base pair radical ions: effect of base pairing on proton-transfer energies, electron with atomic and molecular solids, scanning Microsc. **9**, 619-656 (1995).
- <sup>12</sup> For vertical electron attachment energies in gas phase nucleobases below 5 eV see K. Aflatooni, G. A. Gallup, P. D. Burrow, *J. Phys. Chem.* A102, 6205 (1998); for detachment energies in solvated uracil cluster anions see J. H. Hendricks, S. A. Lyapustina, H. L. de Clercq, K. H. Bowen, *J. Chem. Phys.* 108, 8 (1998).
- <sup>13</sup> Stepanovic M., Pariat Y., and Allan M. Dissociative electron attachment in cyclopentanone, g-butyrolactone, ethylene carbonate, and ethylene carbonate-d4: role of dipole-bound resonances. *J. Chem. Phys.* 11376-11382 (1999).
- <sup>14</sup> Huels M.A.; Abdoul-Carime H.; Illenberger, E.; Sanche L., in preparation.
- <sup>15</sup> Abdoul-Carime Huels, M.A.; Illenberger, E.; Sanche L., in preparation.
- <sup>16</sup> Rowntree, P., Parenteau, L., and Sanche, L., Electron stimulated desorption via dissociative attachment in amorphous H<sub>2</sub>O, *J. Chem. Phys.*, 94,8570-8576 (1991).
- <sup>17</sup> Rowntree P., Parenteau L., and Sanche L., *J. Phys. Chem.* 95, 4902 (1991).
- <sup>18</sup> A. D. Bass, L. Parenteau, M. A. Huels, and L. Sanche, *Reactive Scattering of O<sup>-</sup> in Organic Films at Sub-Ionization Collision Energies*, *J. Chem. Phys.* **109**, 8635 – 8640 (1998).
- <sup>19</sup> Abdoul-Carime H.; Dugal P-C. and Sanche L., Damage induced by 1-30 eV electrons on Thymine- and Bromouracil-substituted oligonucleotides. *Radiation Research* 153, 23-28 (2000).

#### **IV. CONCLUSIONS GÉNÉRALES**

La plupart des dommages de l'ADN irradié sont attribués à la formation de charges négatives ou positives et aux réactions de radicaux  $\cdot\text{OH}$ . Or, on sait que  $\sim 30\%$  de l'énergie des particules primaires est absorbée en excitations moléculaires non ionisantes du milieu, l'autre  $70\%$  produisant l'ionisation (Srdoc *et al.*, 1995). Cobut et collaborateurs (1998) ont démontré récemment par un calcul Monte-Carlo que, pour des électrons incidents de 20 keV dans l'eau liquide, une large production d'électrons secondaires éjectés (88%) a une énergie inférieure à 20 eV. Il est donc crucial d'essayer de comprendre et de savoir où va l'énergie de ces électrons secondaires et des excitations moléculaires et de quelle façon cette énergie contribue-t-elle au dommage de l'ADN?

On sait maintenant (Michaud et Sanche, 1987; Rowntree *et al.*, 1991) qu'une partie de l'énergie des électrons secondaires sert à produire des radicaux  $\cdot\text{OH}$ , mais, plusieurs autres réactions dans le domaine de la femtoseconde restent encore inconnues. Des études directes sur des systèmes condensés simples démontrent que les dommages dus aux électrons secondaires mettent en jeu ou produisent la dissociation moléculaire. En effet, des études d'impact électronique réalisées récemment dans notre laboratoire sur la dégradation des bases de l'ADN (Huels *et al.*, 1998) et de systèmes organiques simples (Dugal *et al.*, 1999; Rowntree *et al.*, 1996; Leclerc *et al.*, 1987) montrent que les électrons de faible énergie (0-30 eV) produisent facilement des bris moléculaires dans des films minces de ces molécules. En se basant sur les différentes études citées ci dessus, un effort important a été mené dans le présent travail afin d'étudier l'effet de ces particules sur l'ADN isolé et de comprendre de quelle façon ces particules contribuent-elles au dommage de l'ADN. Ceci pourrait nous ouvrir une avenue originale permettant de mieux

appréhender les aspects mécanistiques et réactionnels sur lesquels reposent la formation des dommages induits dans l'ADN irradié.

Nous avons pu démontrer par le biais de ce travail que des techniques d'ultra-vide combinées à des méthodes standards de biologie peuvent être utilisées pour mesurer les dommages directement induits à la molécule d'ADN isolé, par impact d'électrons de faible énergie (3 – 1500 eV) .

La première section de nos résultats montrent que les électrons secondaires d'énergie comprise entre 100 et 1500 eV induisent des dommages biologiques importants, à savoir des coupures simple, double et multiple dans la molécule d'ADN. Nous avons en effet, observé une augmentation marquée dans l'efficacité d'induire des coupures double et multiple en fonction de l'énergie des électrons incidents. Et étant donné que ces derniers augmentent plus rapidement que les cassures double brins, ceci suggère que certains mécanismes de dommages produisent directement des cassures multiples après un simple impact d'électron. Ceci est vraisemblablement le résultat du parcours des électrons qui augmente avec leur énergie en leur donnant une plus grande probabilité d'interaction avec plusieurs sections de l'ADN, qui donnent lieu à des sites de dommages multiples locaux.

La deuxième section de notre étude a été faite à plus basse dose et à plus basse énergie, dans laquelle les résultats démontrent que les électrons secondaires, même à des énergies bien plus basses que le seuil de l'ionisation de l'ADN (8 – 10 eV) induisent des rendements significatifs de cassures simple, double et multiple qui sont causées par un attachement de l'électron incident sur les différents composants de l'ADN (phosphate,

sucres, bases ou H<sub>2</sub>O) qui mène à la formation d'une résonance, (formation d'un état d'anion moléculaire transitoire (AMT) de courte vie) (Schulz, 1973) suivis par une rupture de liens et de réactions subséquentes des produits de fragmentation dans un petit volume formant des sites de dommages multiples et des lésions sur les brins opposés. Ce qui contredit fondamentalement les notions traditionnelles qui suggèrent que le dommage induit par les électrons secondaires sont produits uniquement à des énergies supérieures à celles de l'ionisation, ou alors par la réaction des espèces chimiques formées après la solvataion de ces électrons.

Il est intéressant de noter que le dommage de l'ADN induit par les électrons est très sensible à l'énergie cinétique initiale de l'électron, particulièrement au dessous de 15 eV, où on a observé un seuil à 3 – 5 eV avec la présence d'un épaulement à 5.5 - 6 eV pour les rendements des cassures simple brin, probablement relié à quelques canaux de fragmentation observés avec la cytosine et la thymine en phase gazeuse au dessous de 10 eV (Huels *et al.*, 1998) (ou encore des canaux de fragmentation dans l'adénine ou la guanine). On a observé aussi un pic important à 10 eV qui reflète une claire signature de la résonance (Schulz, 1973). Ceci est totalement différent des lésions de brins d'ADN induites par des photons à des énergies similaires, où, l'induction des cassures simple et double brins augmente de façon monotone au dessus du seuil de l'ionisation de 7 eV et demeure constante entre 12 et 100 eV (Hieda, 1994; Michael, 1995).

L'augmentation continue des rendements de coupures simple, double et multiple observée au dessus de 15 eV, est principalement due aux mécanismes non résonants comme l'ionisation suivie par des dissociations des ions positifs excités et/ou des dissociations dipolaires (i.e. fragmentation en ions positifs et négatifs). Ceci a été observé

dans plusieurs études sur l'impact des électrons de faible énergie sur différentes molécules d'intérêt biologique (ex., des analogues de sucre (Antic *et al.*, 1999), des bases de l'ADN (Huels *et al.*, 1998), des homo-oligomères (Dugal *et al.*, 1999), H<sub>2</sub>O (Rowntree *et al.*, 1991) qui ont démontré une augmentation continue des rendements de fragmentations à des énergies supérieures à 15-20 eV, attribuée aux mécanismes non résonants.

En se basant sur ces estimations et en prenant en considération la distribution des électrons secondaires émis par la radiation primaire calculée par Cobut *et al.*, on peut s'attendre à ce que le dommage induit par les électrons d'énergie < 20 eV, serait encore plus dramatique et plus amplifié que le dommage mesuré dans le présent travail. En effet, Abdoul-Carime *et al.*, ont démontré que la probabilité d'induire des fragmentations dans des oligonucléotides par impact d'électrons de 13 eV, est trois fois plus élevée lorsqu'on prend en considération la distribution des électrons secondaires (Abdoul-Carime *et al.* 2000).

Un phénomène très intéressant a été observé et qui reste à exploiter et à étudier concernant la forte décroissance des cassures doubles mais pas des cassures simple brins à 13 eV. Ce mécanisme semble être une signature de l'interférence qui est particulièrement sensible à la phase condensée et spécialement quand la longueur d'onde de l'électron est du même ordre que la distance entre molécules ou les atomes des diffuseurs (plus spécifiquement dans un solide ordonné). On peut remarquer que la distance entre les bases de l'ADN (3.4 Å) correspond étrangement à la longueur d'onde de l'électron à 13 eV comme indiqué dans la figure 6.1. Cependant, ceci nécessite plus

d'investigations et représente un nouveau phénomène qui mérite de plus amples développements.

Ce travail met donc en relief l'importance de l'interaction des électrons avec le milieu biologique. En effet, nos mesures montrent clairement que les mécanismes de dommage de l'ADN induits par les électrons de basse énergie sont significativement différents de ceux des photons UV ou VUV, et que le dommage ne dépend pas seulement de la quantité d'énergie déposée, mais aussi de la nature physique de l'espèce secondaire qui dépose l'énergie.

Nos résultats démontrent que les électrons secondaires de faible énergie produits en grand nombre par les radiations, et particulièrement la réaction de leurs produits, jouent un rôle crucial dans la radiolyse de l'ADN à des temps très courts, puisqu'ils induisent des dommages significatifs bien avant leur thermalisation et bien avant le début de la diffusion des espèces réactives secondaires produites le long des traces de la radiation ionisante. On remarque qu'en plus des excitations et dissociations non résonantes, des mécanismes de résonance tel que l'attachement dissociatif, contribuent aux dommages de l'ADN.

Étant donné que le type d'interaction fondamentale électron-molécule, observée dans tous les travaux effectués dans notre laboratoire, semble se produire dans de petites molécules quelque soit le milieu dans lequel ils résident, il serait possible que ce soit aussi le cas dans la cellule vivante, et constitue ainsi un phénomène très important, non reconnu auparavant, dans la génotoxicité des radiations.



Il serait important de continuer des recherches dans la même direction et d'essayer de déterminer expérimentalement plus précisément la distribution des électrons secondaires en fonction de l'énergie dans un milieu biologique afin de savoir combien d'électron secondaire ayant des énergies de 3 à 10 eV pourraient être générés par la radiation primaire dans le voisinage de l'ADN cellulaire. Ceci nous permettrait de combler l'immense lacune qui existe sur l'interaction des radiations avec la matière ainsi que le manque d'informations fondamentales qui nous permettraient de mieux comprendre les événements ultra-rapides induits au niveau moléculaire par les électrons de basse énergie afin d'acquérir une description microscopique des dépôts d'énergie. Ce qui nous aiderait certainement à mieux cerner le problème de la radioprotection et l'importance de la radiosensibilisation, sachant que l'incorporation de bases halogènes (telle que le Bromo-uracile) à l'ADN, accroît la sensibilité de certaines cellules aux rayonnements ionisants (Cadet et Vigny, 1989).<sup>2</sup>

---

<sup>2</sup> Récemment, Abdoul-Carime *et al*, ont mesuré un rendement de fragments 3 fois plus élevé lorsque des halodésoxyuridines sont incorporés dans des hlogonucléotides (Abdoul-Carime *et al*, 2000)

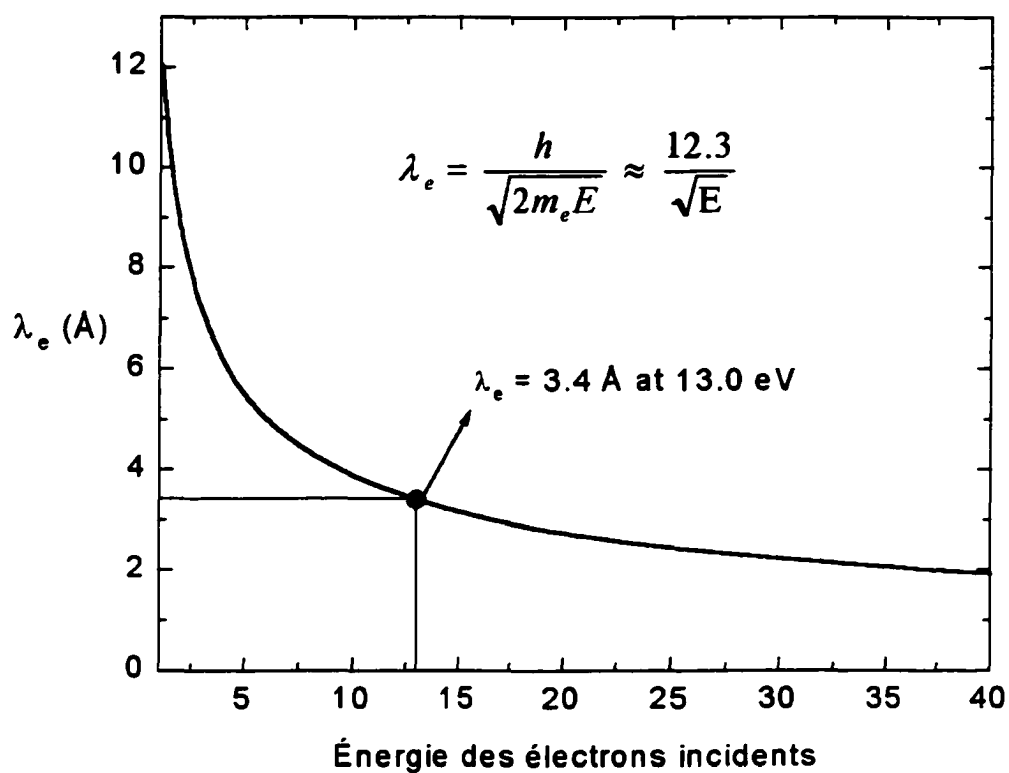


**Figure 6.1 :** Longueur d'onde de l'électron DeBroglie (en Å) en fonction de l'énergie des électrons incidents  $E$  (en eV).

***Et oui c'est terminé! Incroyable... mais vrai!***

## **REMERCIEMENTS**

J'aimerais exprimer mes remerciements les plus sincères et les plus profonds à Maman et Papa... Merci d'être si compréhensifs, et merci de m'avoir tant encouragé et soutenu dans tous les choix que j'ai pu faire dans la vie.

Merci à mes très chers sœurs et frères, Soumia, Malika, Mourad et Réda, sans oublier mes trois petits choux, la grande Nessrine, l'adorable Sofène et la petite puce Inès.

Merci à vous tous d'être tout simplement ce que vous êtes pour moi... *le rayon de soleil qui éclaire ma vie et mon existence quotidiennement et à n'importe quelle heure de la journée.*

Je tiens à remercier très chaleureusement mes codirecteurs Léon Sanche et Darel Hunting pour la supervision de mon projet. Merci pour ta grande modestie et ta sympathique complicité Léon. Merci pour ta gentillesse et ta sensibilité Darel.

Merci Mickael Huels d'avoir été mon grand conseiller pour la rédaction de mes articles et merci d'avoir accepté de présider ma soutenance.

Un grand MERCI à vous Jean Cadet d'avoir accepté pour la 2ème fois de faire le déplacement, pour moi, de Grenoble à Sherbrooke. Je suis fière d'avoir parmi les membres de mon jury, un pionnier du dommage des acides nucléiques.

Merci, Guylain Boissonneault, d'avoir accepté d'être membre de mon jury de thèse.

Merci à mon Héro, Pierre Cloutier. Merci pour ton support technique. Travailler avec toi est un véritable plaisir. Merci de m'avoir écouté et d'avoir été là à chaque fois que j'avais besoin de toi. Merci et encore Mille Merci Pierre, U. R. the BEST.

**Merci Daniel Robillard pour ton support technique en informatique. Merci d'avoir résolu tous mes "bogues". Merci pour ta gentillesse et surtout merci de m'avoir initié au sport national Québécois, le "hockey". Je suis une Pro' maintenant!.**

**MERCI à tous mes merveilleux amis,**

**À commencer par mon Ange Gardien, Isabelle. Merci pour ta grande amitié, ta générosité et tes encouragements inlassables... Je te suis très reconnaissante pour tout.**

**Pascale, Annie, Bertrand, Fouzia, Dominic, Paul, Abdel, Fatiha, Hamid et Zoulikha, vous êtes tout simplement ADORABLES. Merci à vous tous pour l'ambiance chaleureuse et familiale que vous avez su créer autour de moi chacun à votre façon.**

**Je voudrai remercier tous les membres du laboratoire, Sylvain, Pierre, Luc, Marc, Andrew, Hassan... et tous les autres.**

**Merci à mes parents Québécois, Agathe et Jean Ménard. Votre attention, votre gentillesse et votre présence me font chaud au cœur. Merci.**

**Je ne pourrais pas fermer la boucle sans avoir une pensée pour toi Soheir... Te connaissant, je suis sûre que tu aurais été très fière de moi aujourd'hui, comme tu l'as toujours été pour toutes mes autres réussites et tous mes autres diplômes. Merci pour tout très chère AMIE.**

## **RÉFÉRENCES BIBLIOGRAPHIQUES**

- Abdoul-Carime H., Dugal P-C., and Sanche L., 2000, Damage induced by 1-30 eV electrons on Thymine- and Bromouracil-substituted oligonucleotides. *Radiation Research* **153**, 23-28.
- Antic D., Parenteau L., Lepage M., Sanche L., 1999, *J. Phys. Chem.* **103**, 6611.
- Becker D. et Sevilla M.D., 1993, The chemical consequences of radiation damage to DNA, *Adv. Radiat. Biol.* **17**, 121.
- Boudaïffa B., Cloutier P., Hunting D., and Sanche L., Low-energy (3-100 eV) electron damage to DNA, to be published.
- Boudaïffa B., Cloutier P., Hunting D., Huels M. A., and Sanche L., Resonant induction of DNA strand breaks by low energy (3 – 20 eV) electrons, *Science* (2000, in press).
- Boudaïffa B., Cloutier P., Hunting D., Huels M. A., and Sanche L., Induction of single and double strand breaks in plasmid DNA by 100 to 1500 eV electrons. To be published.
- Boudaïffa B., Cloutier P., Hunting D., Huels M. A., Sanche L., Electron Resonance in DNA Induced by Very Low Energy Electrons (3 – 50 eV). To be published.
- Cadet J., Vigny P., 1989, The photochemistry of nucleic acids, in *Bioorganic photochemistry, Photochemistry and the nucleic acids*, Vol 1, edited by H. Morrison.
- Cobut V., Frongillo Y., Patau J. P., Goulet T., Fraser M.-J., et Jay-Gérin J.-P. 1998, Monte Carlo simulation of fast electron and proton tracks in liquid water-I. Physical and physicochemical aspects. *Radiation Physics and Chemistry* **51**, 229.

- Dugal, P. C.; Huels, M. A.; Sanche, L., 1999, Low-energy (5-25 eV) electron damage to homo-oligonucleotides, *Radiation Research.*, **151**, 325-333.
- Faraggi M., Ferradini C., Jay-Gérin J.-P., 1995, Migration et devenir des charges formées initialement dans l'ADN irradié : une synthèse. *New Journal of Chemistry* **19**, 1203-1215.
- Hieda K., 1994, DNA damage induced by vacuum and soft X-ray photons from synchrotron radiation. *Int. J. Radiat. Biol.* **66**, 561-567
- Huels M.A., Hahndorf I., Illenberger E. et Sanche L., 1998, Resonant dissociation of DNA bases by subionization electrons, *J. Chem. Phys.*, **108** (4), 1309-1312.
- Hutchinson F., 1954, Energy requirements for the inactivation of bovine serum albumin by radiation. *Radiat. Res.* **1**. p. 43.
- Leclerc G., Cui Z. et Sanche L., 1987, "Effective dissociation cross section for the low-energy (0.5-31 eV) electron impact on solid *n*-hexane thin films", *J. Phys. Chem.* **91**, 6461.
- Michael B. D., Prise K. M., Folkard M., Vojnovic B., Brocklehurst B., Munro I. H., and Hopkirk A., 1995, in *Radiation damage in DNA: Structure/function relationships at early times*. (eds. Fuciarelli, A. F., Zimbrick, J. D.) 251-258 (Battelle Press, Columbus, OH).
- Michaud M. et Sanche L., 1987, "Total cross sections for slow-electron (1-20 eV) scattering in solid H<sub>2</sub>O", *Phys. Rev. A* **36**, 4672.
- Michaud M., Cloutier P., and Sanche L., 1991, Low-energy electron-energy-loss spectroscopy of amorphous ice: electronic excitations. *Physical Review A* **44**, 5624.

- Nikjoo H. and Goodhead D. T., 1991, Track structure analysis illustrating the prominent role of low-energy electrons in radiobiological effects of low-LET radiations, *Physics in Medicine and Biology*, **36**, N° 2, 229-238.
- Rowntree P., Dugal P.-C., Hunting D. et Sanche L., 1996, "Electron stimulated desorption of H<sub>2</sub> from chemisorbed molecular monolayers", *J. Phys. Chem.* **100**, 4546.
- Rowntree P., Parenteau L. et Sanche L., 1991, "Electron stimulated desorption via dissociative attachment in amorphous H<sub>2</sub>O", *J. Chem. Phys.* **94**, 8570.
- Sanche L., 1991, Primary interactions of low energy electrons in condensed matter, In *Excess Electrons in Dielectric Media*, edited by C. Ferradini and J. P. Jay-Gerin (Boca Raton: CRC Press, Inc.), pp. 1-42.
- Schultz G. J., 1973, Resonances in electron impact on atoms. *Review of Modern Physics*, **45**, n°3, 378-422.
- Srdoc D., Inokuti M. et Krajcar-Bronic', I. 1995, "Yields of ionization and excitation in irradiated matter", dans "*Atomic and Molecular Data for Radiotherapy and Radiation Research*", IAEA-TECDOC-799 (International Atomic Energy Agency, Vienna), p. 547.
- Swarts, S. G., Sevilla, M. D., Becker, D., Tokar, C. J. and Wheeler, K. T., 1992, Radiation-induced DNA damage as a function of hydration 1. Release of unaltered bases. *Radiation Research*, **129**, 333-344.